GEO-CAPE Methane Working Group

Daniel Jacob (Harvard), David Edwards (NCAR), Kevin Bowman (JPL), Stan Sander (JPL)
Daven Henze (U. Colorado)

Focus: define the specifications for the GEO-CAPE infrared instrument (GCIRI) to provide fine-scale information on methane emissions

Capabilities of different satellite observing systems for mapping methane emissions on regional to km scales

Daniel Jacob, Jianxiong Sheng, Alex Turner, Dan Cusworth

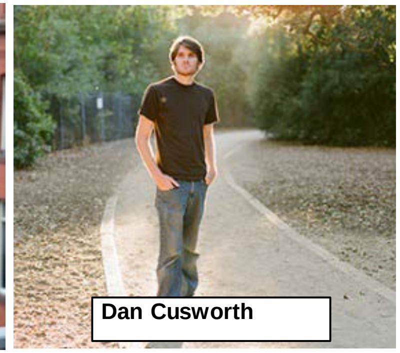

HARVARD UNIVERSITY
ATMOSPHERIC CHEMISTRY MODELING GROUP

- Jacob, D.J., A.J. Turner, J.D. Maasakkers, J. Sheng, K. Sun, X. Liu, K. Chance, I. Aben, J. McKeever, and C. Frankenberg, *Satellite observations of atmospheric methane and their value for quantifying methane emissions*, Atmos. Chem. Phys.,16, 4371-4396, doi:10.5194/acp-16-14371-2016, 2016.
- Turner, A.J., D.J. Jacob, J. Benmergui, J. Brandman, L. White, and C.A. Randles, *Assessing the capability of different satellite observing configurations to resolve the distribution of methane emissions at kilometer scales*, Atmos. Chem. Phys., in press, 2018.
- Sheng, J.-X., D.J. Jacob, J.D. Maasakkers, Y. Zhang, and M.P. Sulprizio, *Potential of low-Earth orbit (TROPOMI) and geostationary (GeoCARB, GEO-CAPE) satellite instruments for constraining methane emissions on fine regional scales: application to the Southeast US* , submitted to Atmos. Meas. Techn., 2018.
- Cusworth, D.H., D.J. Jacob, A.J. Turner, et al., Detecting anomalous emitters in oil/gas fields by satellite and surface observations of atmospheric methane, to be submitted to Atmos. Chem. Phys., 2018.

Satellite observations of atmospheric methane and their value for quantifying methane emissions (Jacob et al., ACP2016)

Simple mass balance analysis to compare capabilities of different systems:

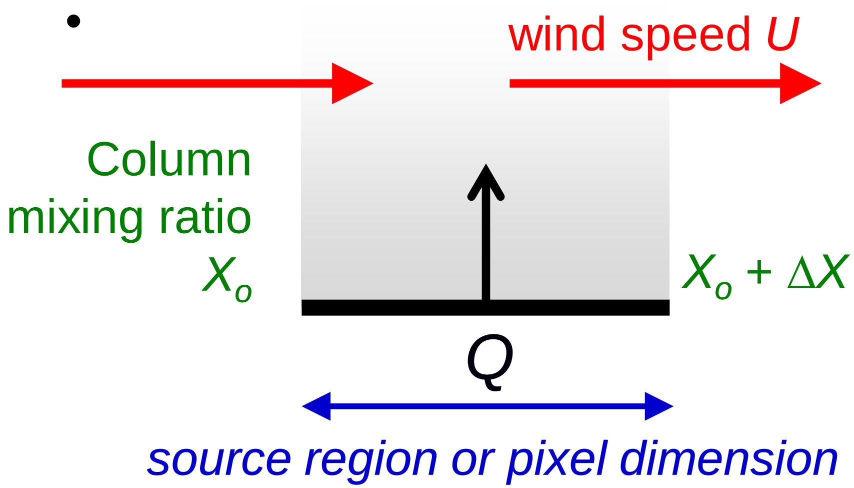

- Pixel resolution
- Return frequency
- Instrument precision

Instrument[a]	Regional source quantification ($Q = 72\,\mathrm{t\,h^{-1}}$ over $300 \times 300\,\mathrm{km^2}$)[b]	Point source detection threshold[c] (Q_{min}, $\mathrm{t\,h^{-1}}$)
SCIAMACHY	1-year averaging time	68
GOSAT	1-year averaging time	7.1
TROPOMI	single pass (1 day)	4.2
GHGSat	NA[d]	0.25[e]
GOSAT-2	4-month averaging time	4.0
MERLIN	7-month averaging time[f]	NA
CarbonSat	single pass (5–10 days)	0.80
GEO-CAPE,	single pass (1 h)	4.0
GeoFTS	single pass (2 h)	0.61[g]
geoCARB	single pass (2–8 h)	4.0
G3E	single pass (2 h)	1.3

Geostationary observations could uniquely detect anomalous emitters by focusing on limited domains with high-frequency observations and high pixel resolution

geo instruments

Regional-scale OSSE for the Southeast US

How does GeoCARB satisfy the GEO-CAPE GCIRI objectives?

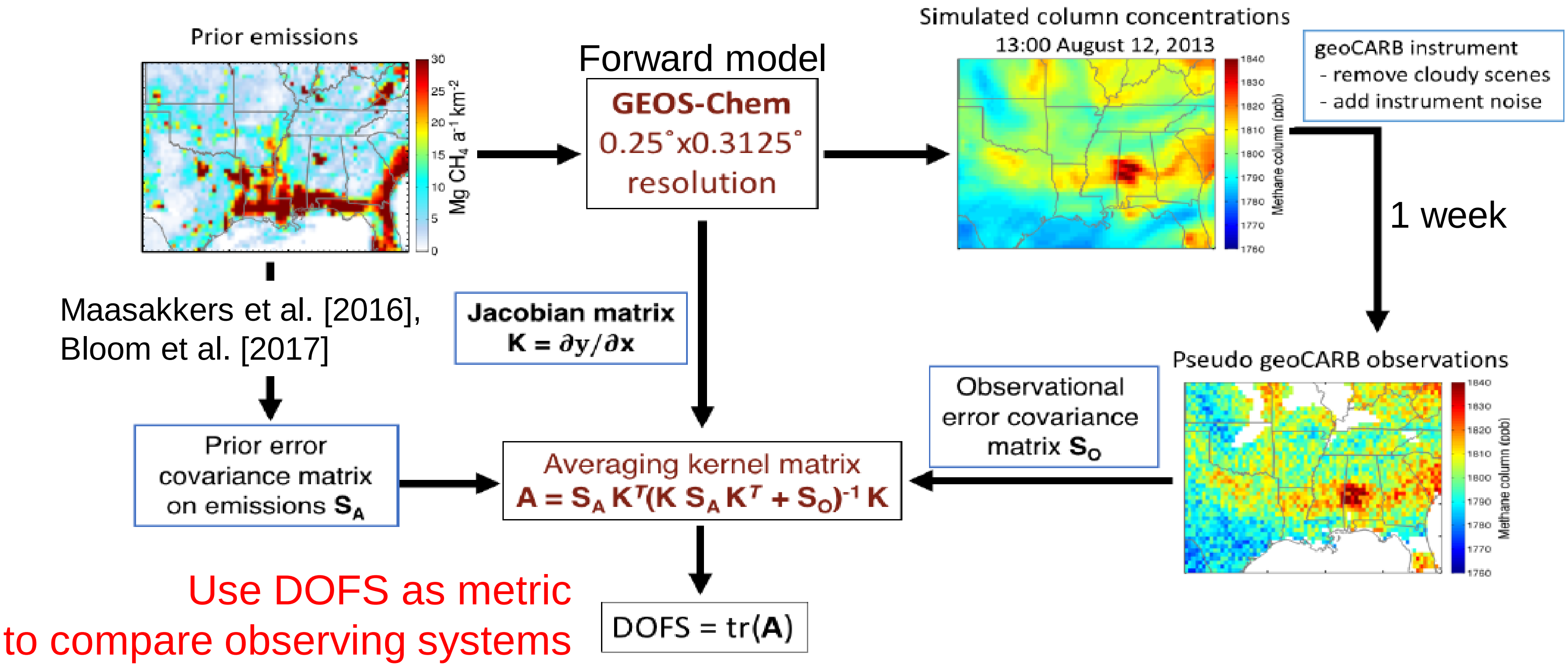

- Cloud mask statistics from Remer et al, (2012) – exclude 73-91% of data depending on pixel size and following GEOS-5 cloud cover
- Forward model column error of 12 ppb, temporal error correlation of 6 hours from GEO-Chem comparison to Lamont TCCON site

Sheng et al. [2018]

Quantifying forward model error statistics with hourly TCCON data

Hourly comparison of 0.25°x0.3125° GEOS-Chem to Lamont TCCON data for Aug-Sep 2013

$$\underbrace{\text{Residual model error}}_{\text{Forward model error}} = \underbrace{X_{CH4,GEOS\text{-}Chem} - X_{CH4,\ TCCON}}_{\text{total error}} - \underbrace{\overline{X_{CH4,GEOS\text{-}Chem} - X_{CH4,\ TCCON}}}_{\text{mean bias (to be corrected by inversion)}}$$

residual error variance

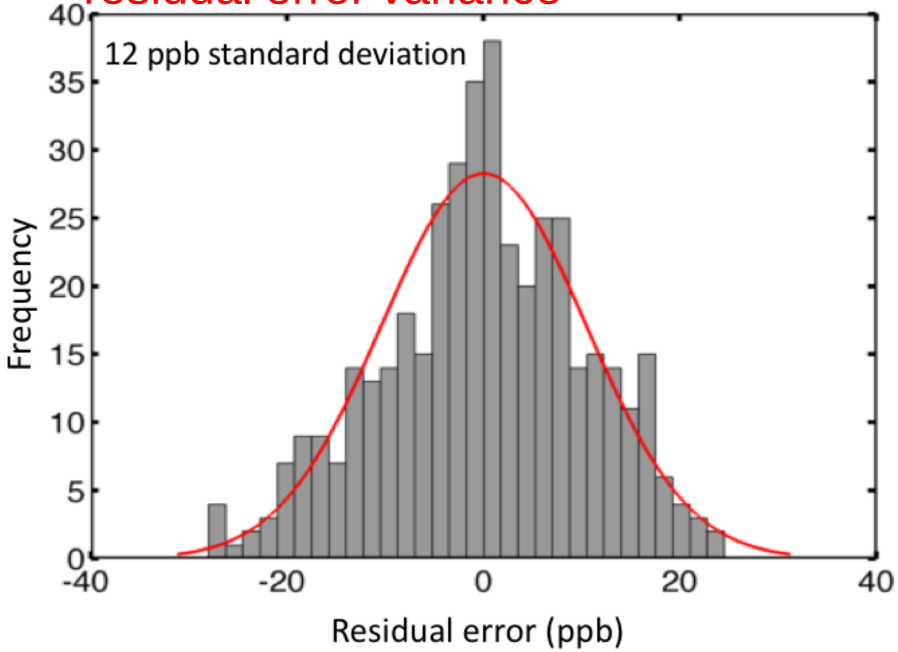

temporal error correlation

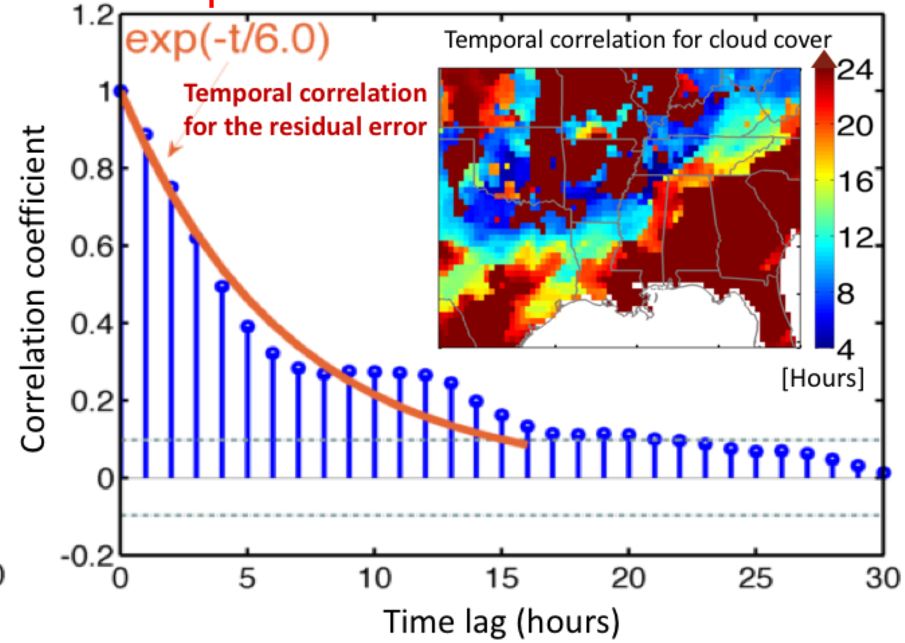

Two key results:

- Forward model error dominates over instrument precision on 25 km scale
- 6-h temporal error correlation diminishes value of frequent return times

Sheng et al. [2018]

Comparing satellite observing systems by their DOFS

Ideal: DOFS=216 (full mapping of 25x25 km^2 emissions)

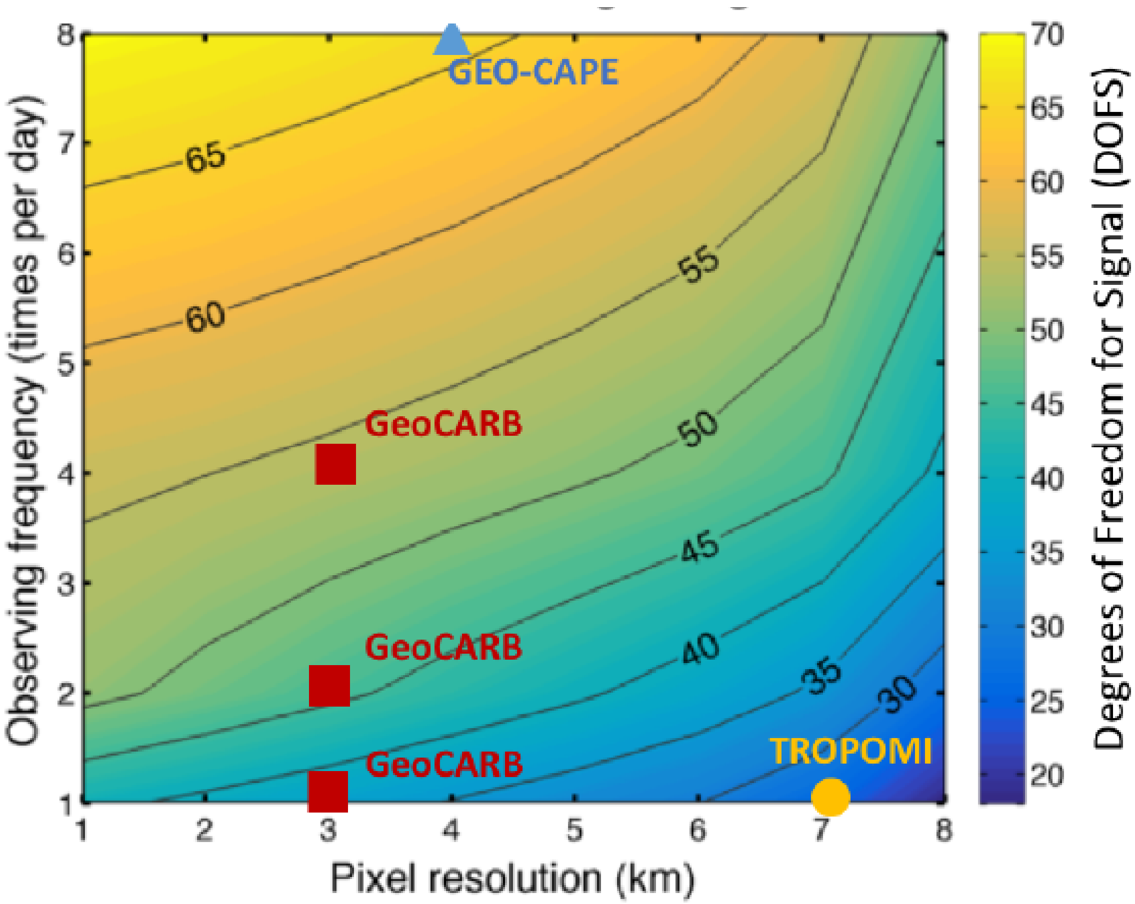

- All systems are better than what SEAC[4]RS aircraft observations could do (DOFS=10)
- GeoCARB 2x/day delivers ~70% of GEO-CAPE (GCIRI) information
- GeoCARB 2x/day performs comparably to alternate schedule of (4x/day, 1x/day)
- TROPOMI is very sensitive to cloud cover, GeoCARB is not

Sheng et al., 2018

Kilometer-scale OSSE over the Barnett Shale

Can GeoCARB and other geo configurations quantify emissions on km scales?

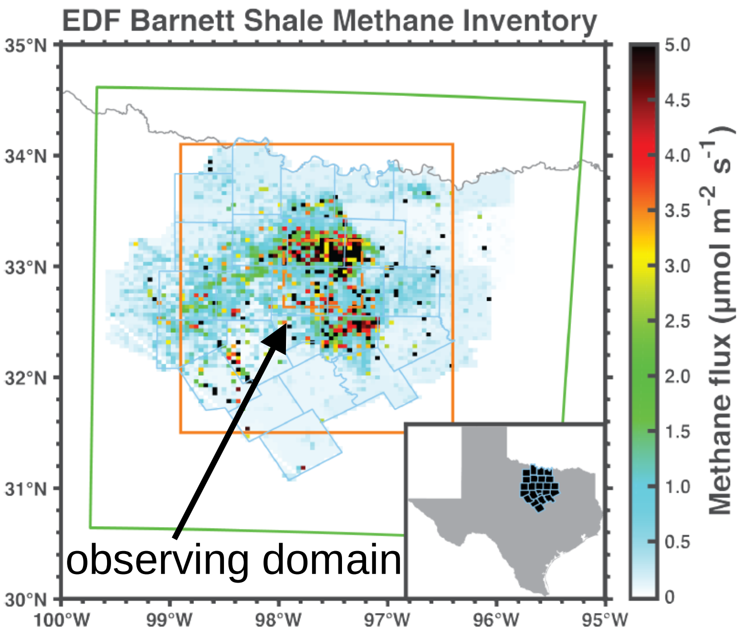

WRF-STILT forward model **K**
(1.3x1.3 km^2 resolution)
1 week (Oct 2013)

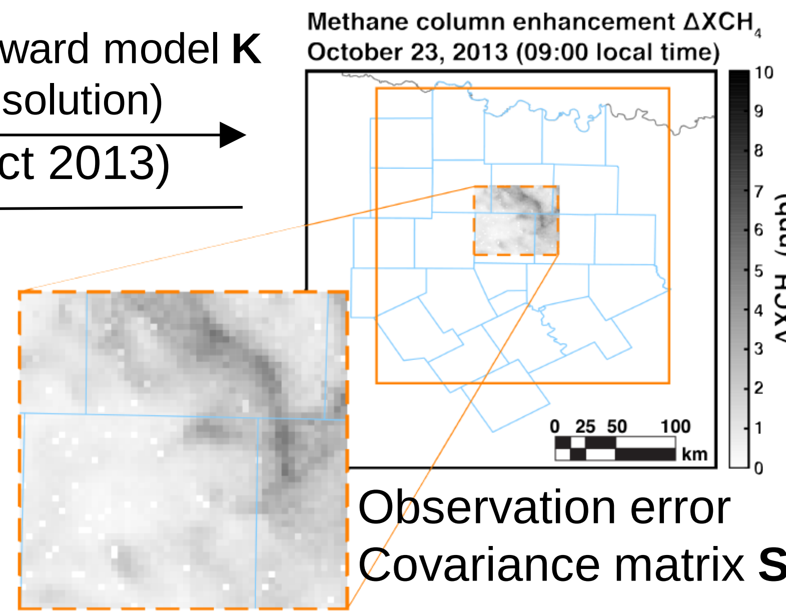

Observation error
Covariance matrix $\mathbf{S_O}$

Lyon et al., 2015

Analyze Fisher information matrix $\mathbf{F} = \mathbf{K}^T\mathbf{S_O}^{-1}\mathbf{K}$

Inverse square roots of eigenvalues of **F** give the methane flux thresholds for detecting the flux patterns described by the corresponding eigenvectors

Turner et al. [2018]

Eigenanalysis of Fisher information matrix

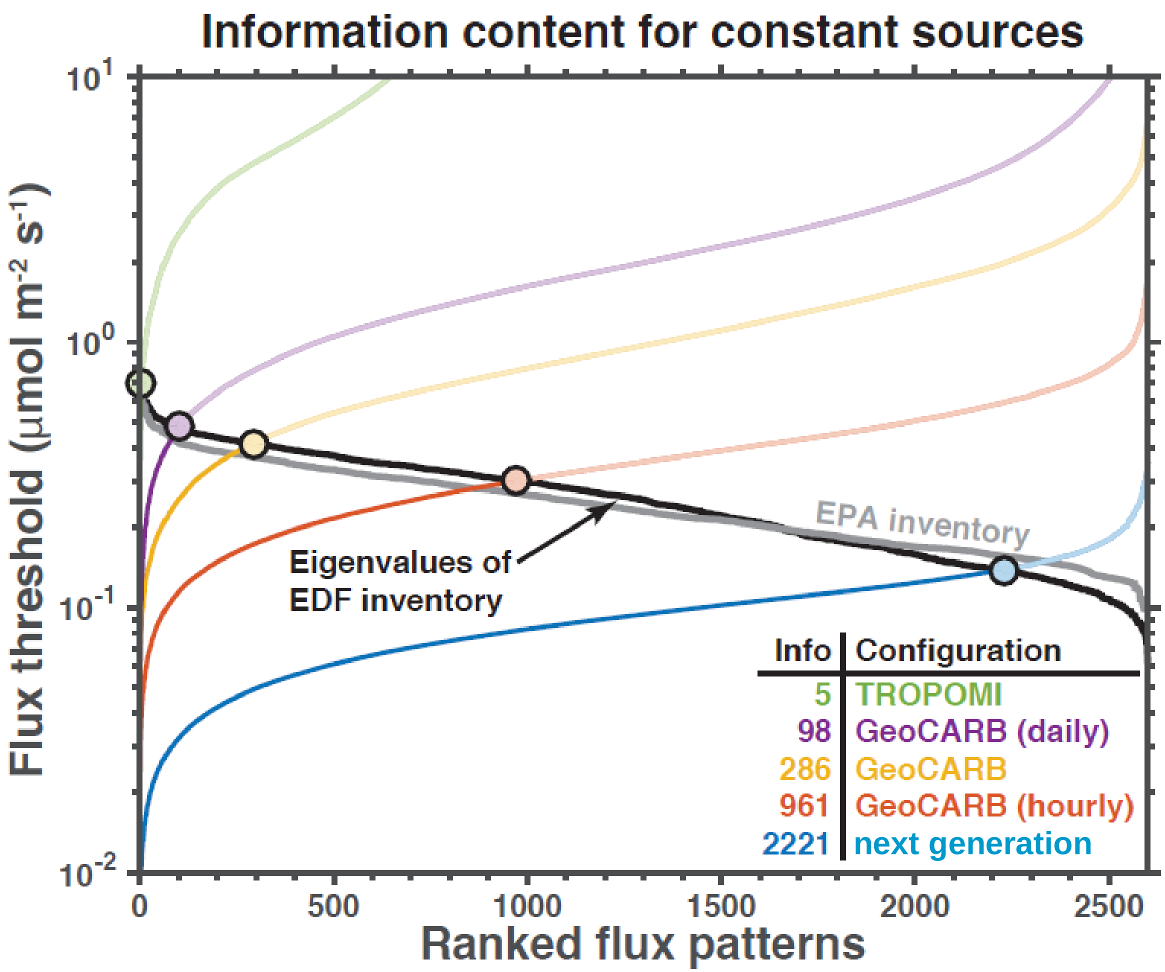

- TROPOMI can achieve ~30 km resolution on emissions in 1 week of observations, GeoCARB can achieve ~2-7 km depending on return frequency
- A next-generation instrument with 1.3x1.3 km^2 pixel resolution, 0.1% precision, hourly return could fully resolve the emission fields

Turner et al. [2018]

On 1-km scale, instrument precision matters more than return frequency

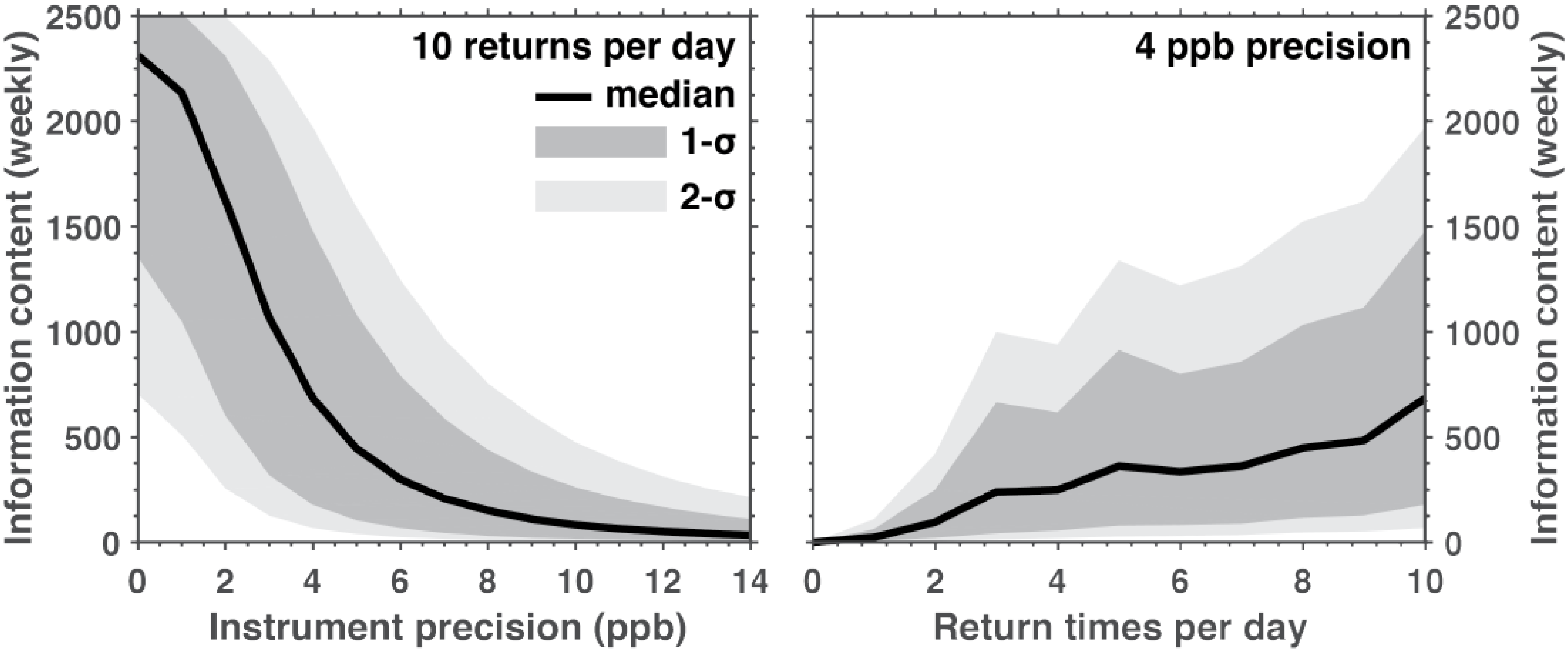

- Instrument precision better than 6 ppb is critical
- Temporal error correlation limits benefit from increasing return frequency

Turner et al. [2018]

Detecting anomalous methane emitters from space

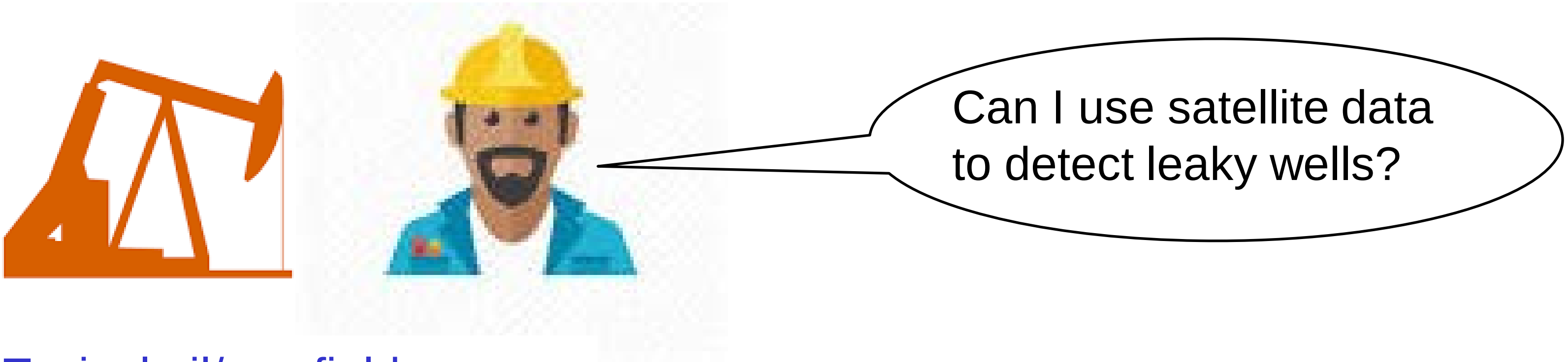

Typical oil/gas field
20-100 wells in 50x50 km^2 domain

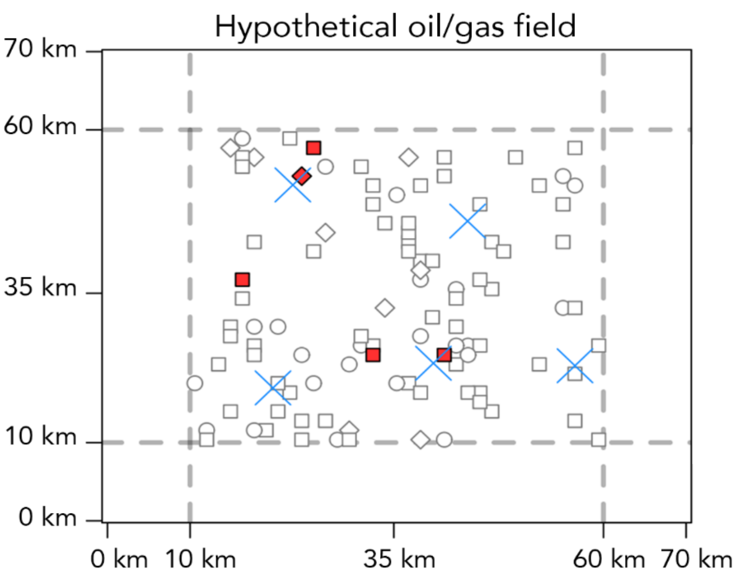

random leaky wells
(high-mode emitters)

bimodal emission pdfs for wells (Barnett Shale, EDF)

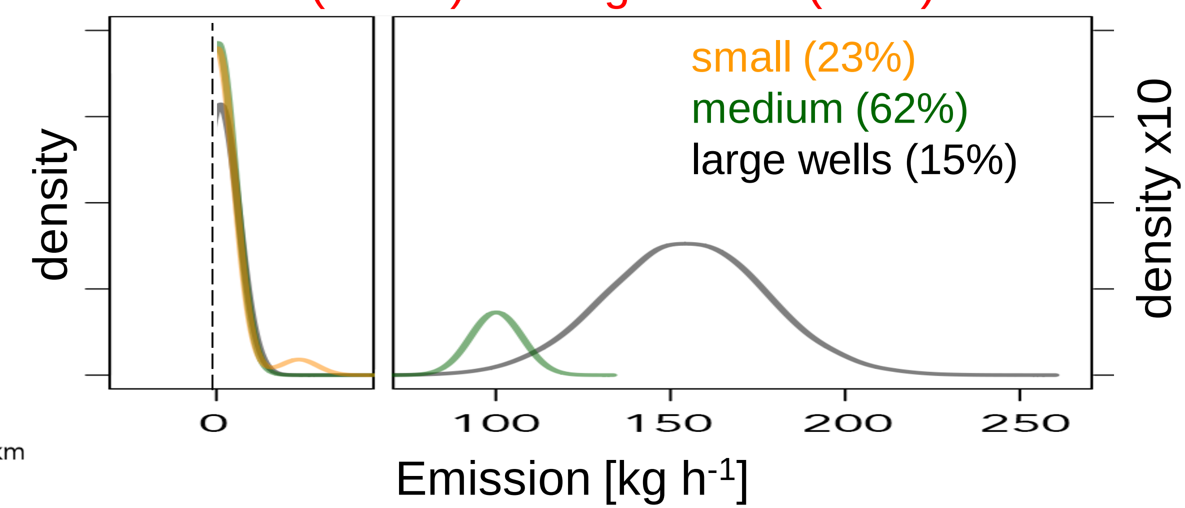

(Cusworth et al., 2018)

OSSE for 50x50 km^2 domain with 20-100 wells

Generate 500 emission scenarios by random sampling of bimodal pdfs

Sample realization (100 wells)

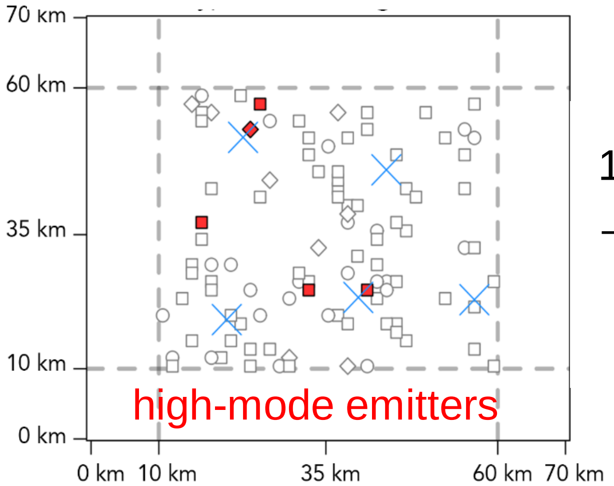

WRF-STILT
1.3x1.3 km^2 resolution

1-week simulation
(Turner et al., 2018)

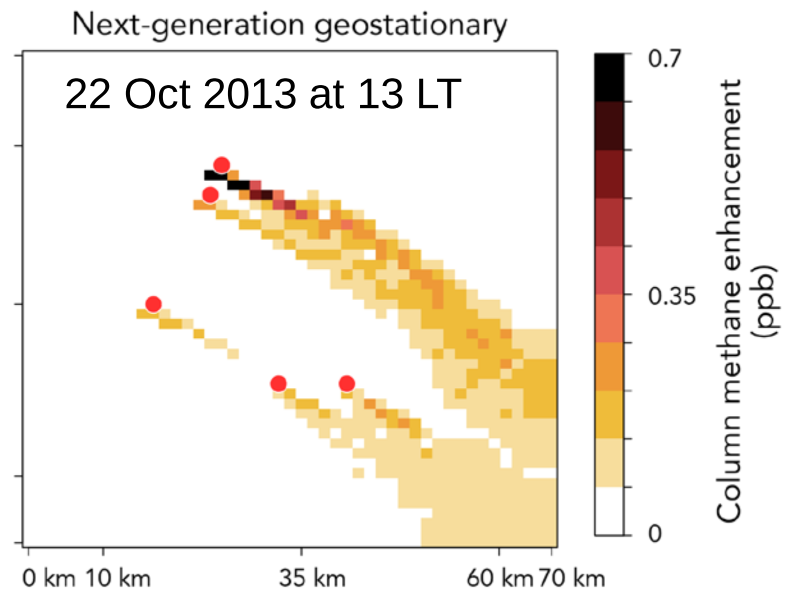

Detection of high-mode emitters by inversion with L-1 regularization (sparse solution):

minimize cost function $J(\mathbf{x}) = (\mathbf{y} - \mathbf{Kx})\mathbf{S}_{\mathbf{O}}^{-1}(\mathbf{y} - \mathbf{Kx})^T + \lambda \|\mathbf{x}\|_1$

with forward model error correlations of 40 km, 2 h

Diagnose success with categorical metrics: T/F for well in high-mode (P) or not (N)

Probability of detection

$$\mathrm{POD}(\%) = 100 \times \frac{\sum \mathrm{TP}}{\sum \mathrm{TP} + \sum \mathrm{FN}}$$

False alarm ratio

$$\mathrm{FAR}(\%) = 100 \times \frac{\sum \mathrm{FP}}{\sum \mathrm{TP} + \sum \mathrm{FP}}$$

Cusworth et al. [2018]

Probability of detection of high-mode emitters (POD) and false alarm ratio (FAR)

Sensitivity to the density of sites (50x50 km^2 domain)

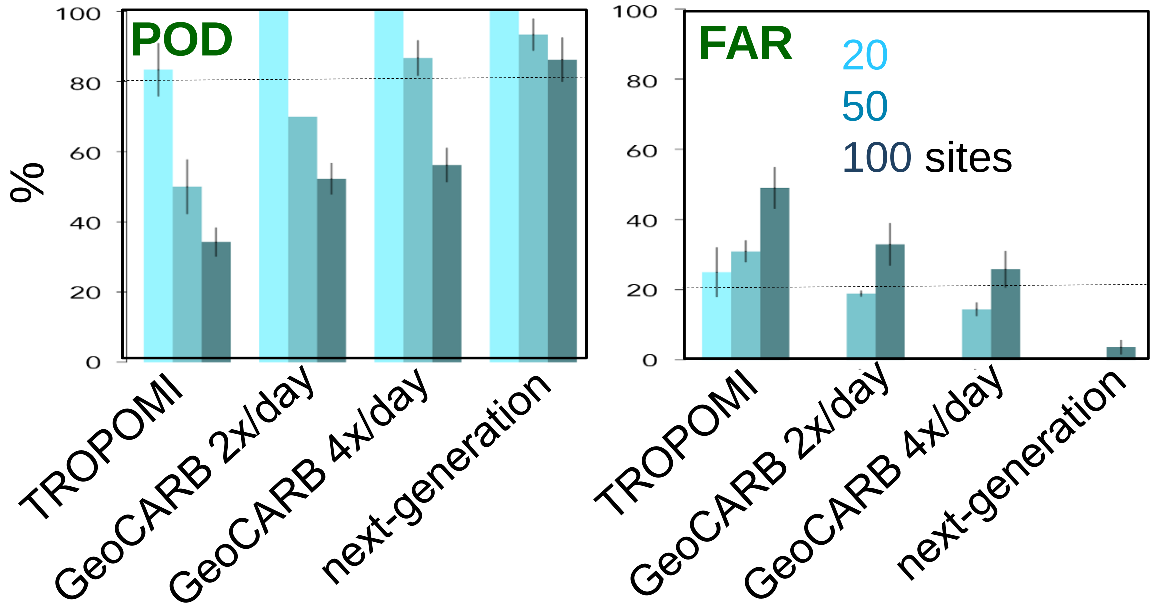

- Problem gets harder as site density increases
- TROPOMI: OK with 20 sites
- GeoCARB 4x/day: 50 sites
- Next-generation: 100 sites

Cusworth et al. [2018]

Can a surface monitoring network complement the satellite data?

5-20 optimally placed surface monitors based on *k*-means of spatial distribution of sites

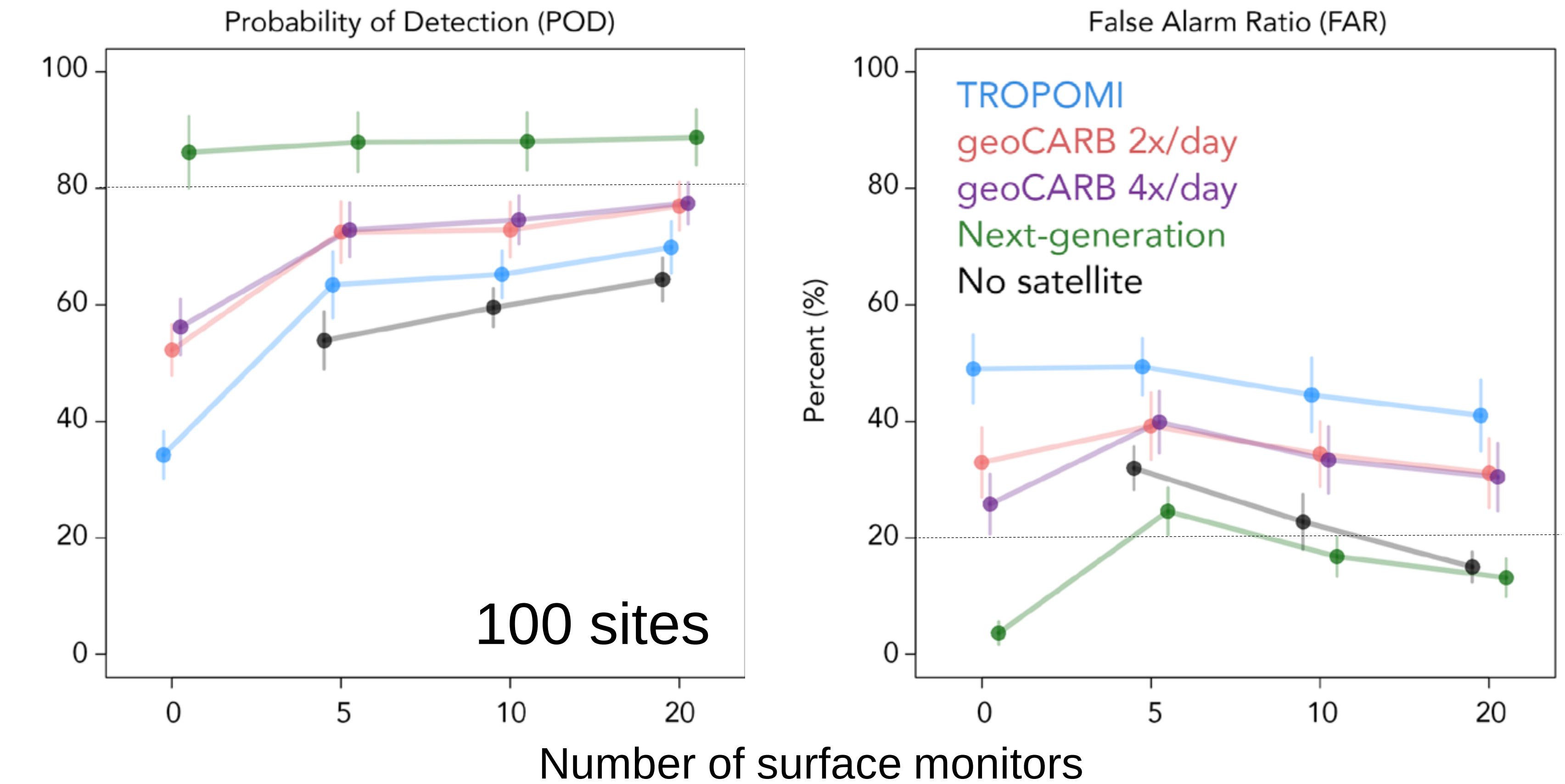

- Surface monitors augment capability of TROPOMI and GeoCARB
- GeoCARB usefully augments a surface network, TROPOMI mostly adds false alarms
- Next-generation satellite does it all – no need for surface monitors

Cusworth et al. [2018]

Findings

- GeoCARB 2x/day delivers about 70% of GEO-CAPE recommendation (GCIRI) for regional mapping of methane sources. Alternating 4x/day and 1x/day gives comparable information to 2x/day
- GeoCARB 2x/day with precision < 6 ppb can map emissions down to 4 km and can detect anomalous emitters in a sparse field of point sources (1 site per 100 km^2)

Recommendations

- A next-generation geostationary instrument with 1.3 km pixel resolution, hourly return, 0.1% precision would be transformative for mapping emissions at km-scale and for detecting anomalous emitters in dense fields
- Instead of the conventional paradigm of using geostationary satellites for continental-scale observations, consider focus on limited domains to enable higher pixel resolution and observation frequency – this would most usefully complement existing LEO capabilities.

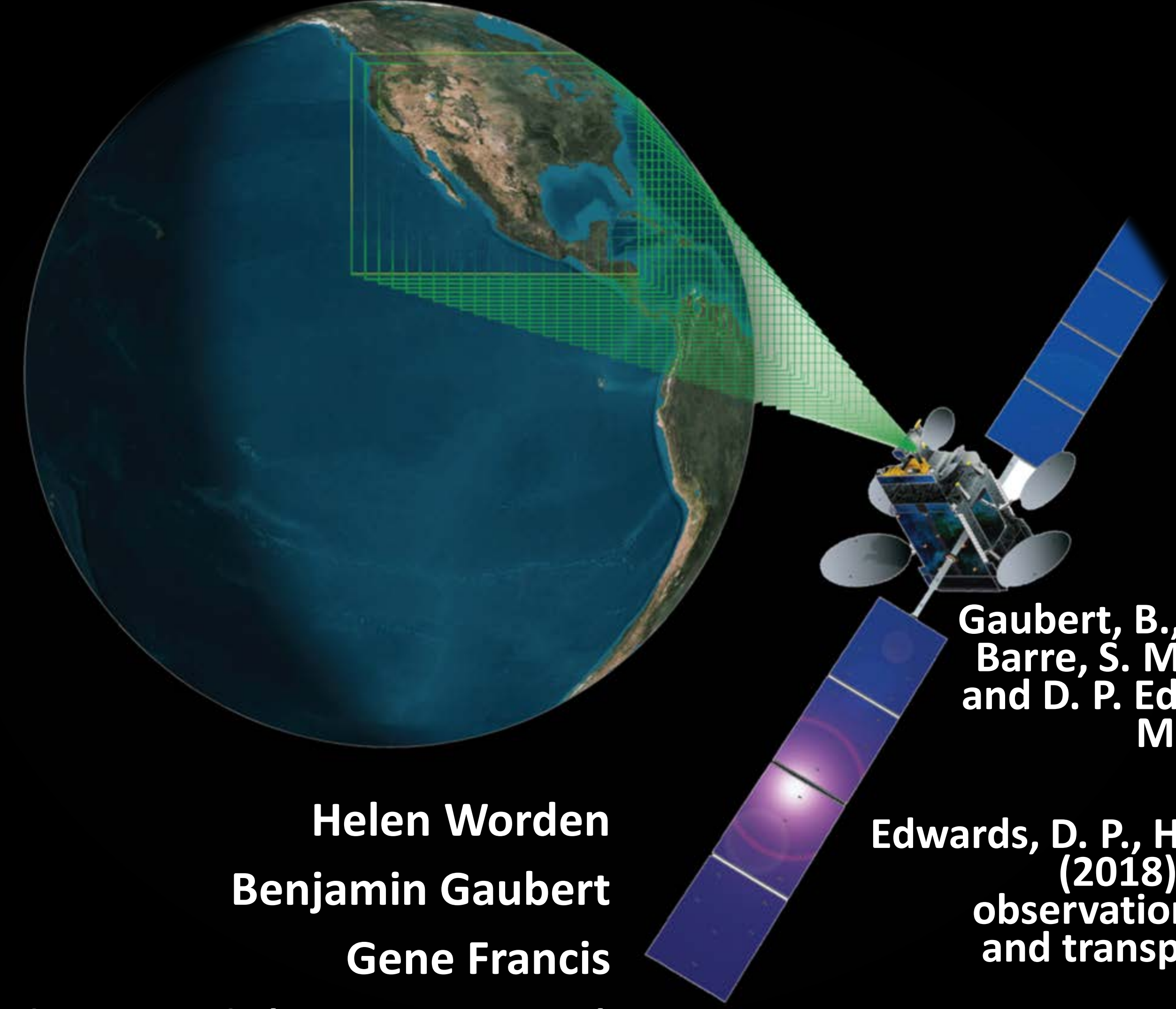

GEOCAPE Methane Working Group: NCAR/ACOM Results

Helen Worden

Benjamin Gaubert

Gene Francis

Jérôme Barré, (now at ECMWF)

Zhe Jiang, (now at USTC)

David Edwards

Publications

Gaubert, B., H. M. Worden, A. F. J. Arellano, L. K. Emmons, S. Tilmes, J. Barre, S. M. Alonso, F. Vitt, J. L. Anderson, F. Alkemade, S. Houweling, and D. P. Edwards (2017), Chemical Feedback From Decreasing Carbon Monoxide Emissions, Geophys. Res. Lett., 44(19), 9985-9995, doi:10.1002/2017GL074987.

Edwards, D. P., H. M. Worden, D. Neil, G. Francis, T. Valle, and A. F. Arellano (2018), The CHRONOS mission: capability for sub-hourly synoptic observations of carbon monoxide and methane to quantify emissions and transport of air pollution, Atmos. Meas. Tech., 11(2), 1061–1085, doi:10.5194/amt-11-1061-2018.

Zhe Jiang, Brian C. McDonald, Helen Worden, John R. Worden, Kazuyuki Miyazaki, Zhen Qu, Daven K. Henze, Dylan B. A. Jones, Avelino F. Arellano, Emily V. Fischer, Liye Zhu, and K. Folkert Boersma (2018), Unexpected slowdown of US pollutant emission reduction in the last decade, Proc. Nat. Acad. Sci. (accepted April, 2018

Facilitating OSSEs: Averaging Kernel (AK) variability
Simulated AK for column CH_4

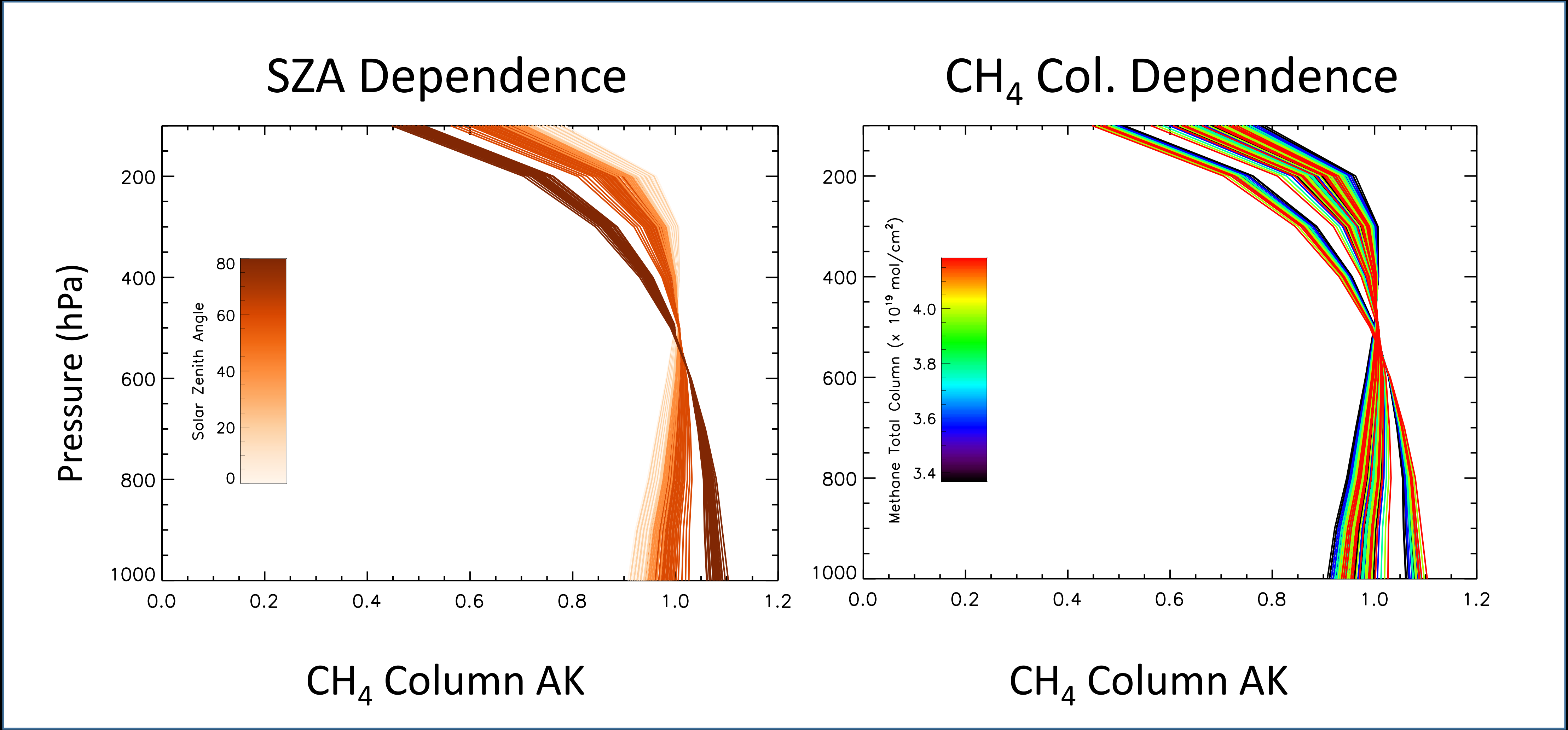

Simulated column CH_4 observations

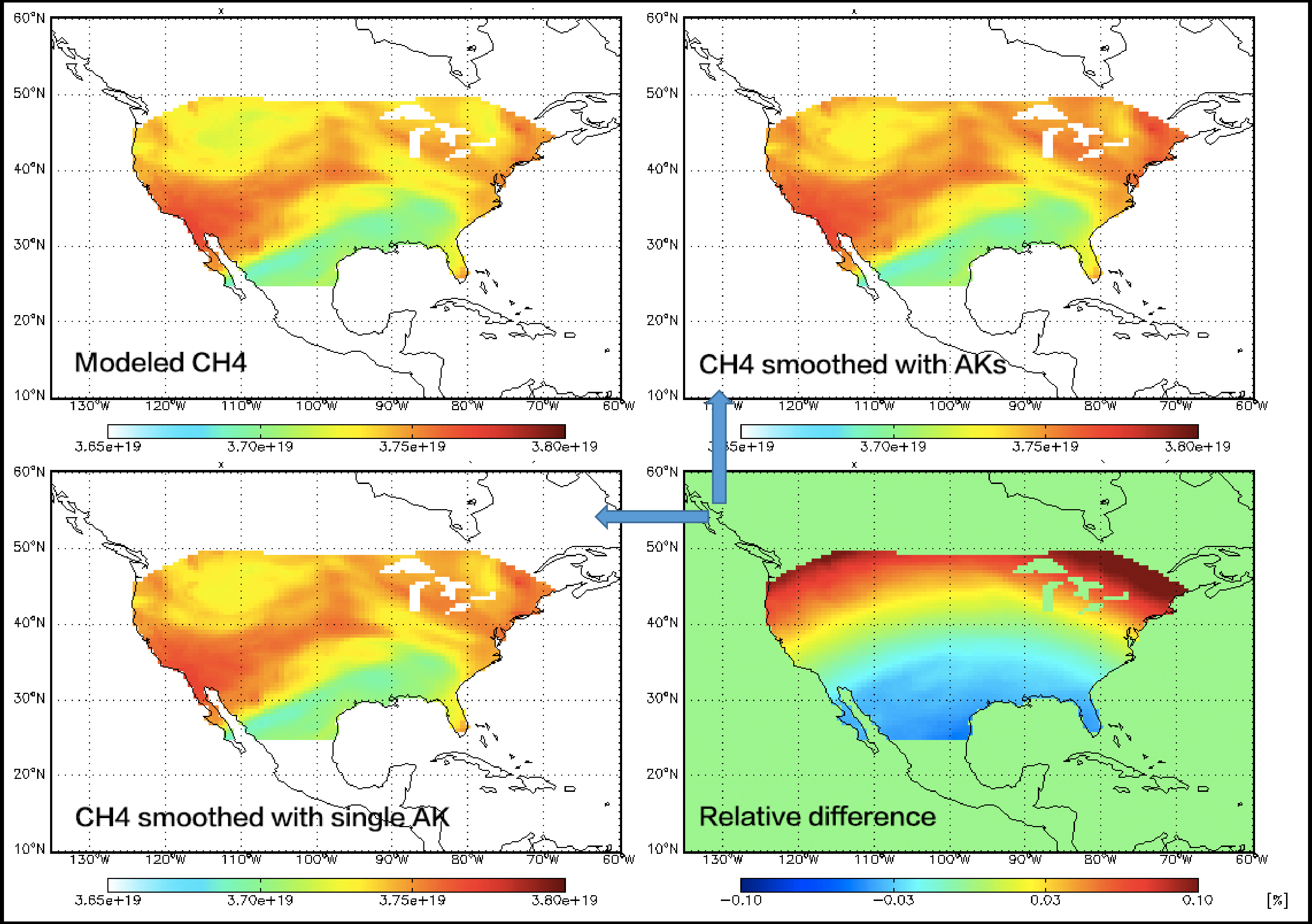

Simulated observations over daylight hours for July 2009

Nature run = GEOS-Chem

- 0.5° x 0.667° resolution
- Full chemistry
- CH_4 emissions from EDGAR v4 and GFED3

Only small ~0.1% differences between simulated observations using scene-dependent CH_4 AKs (LUT) and those using an average AK

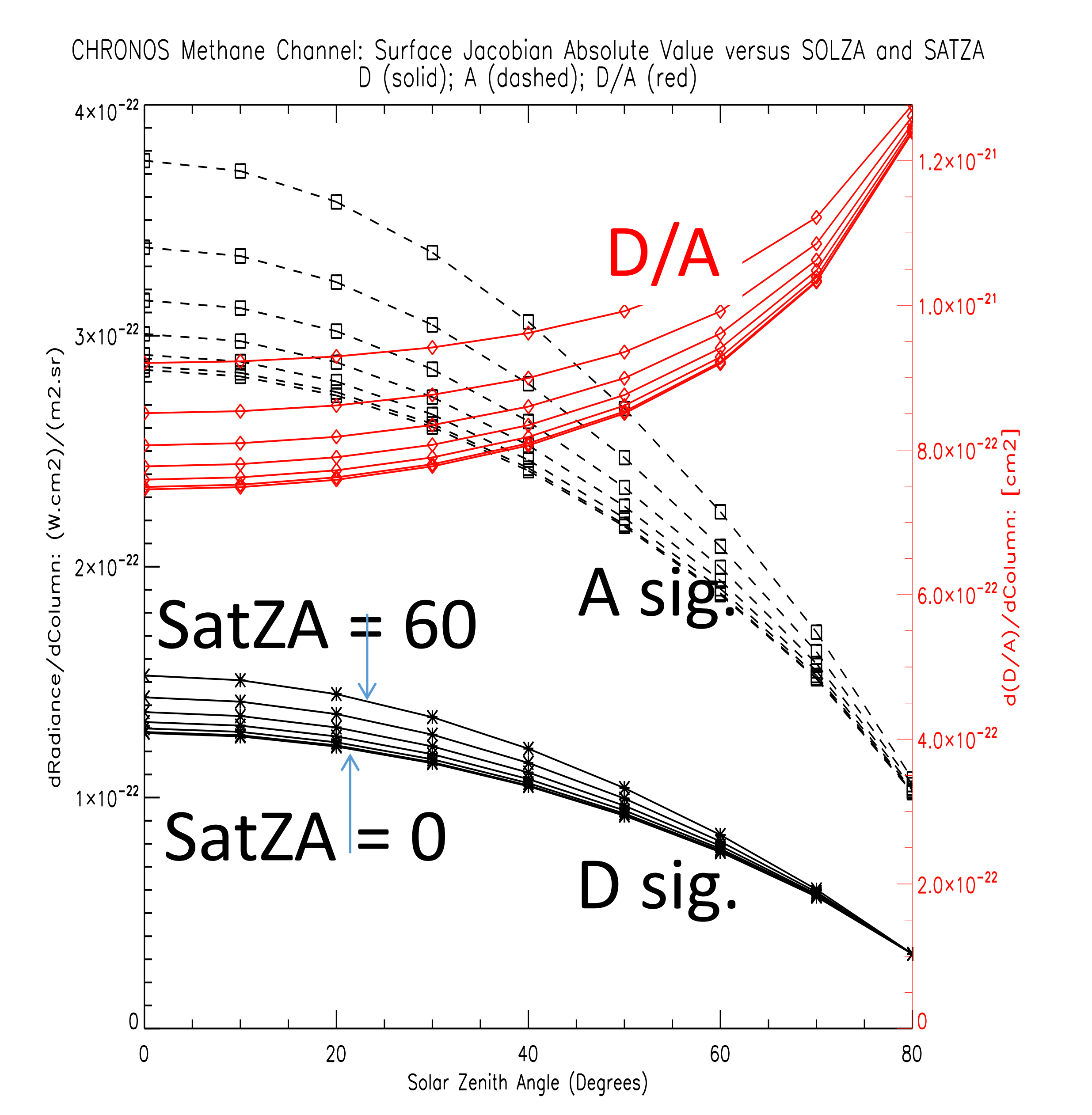

Preparatory studies for the CHRONOS solution for GCIRI:

Analysis of signal dependence on viewing parameters illustrate the GFCR advantage of increased D/A signal at higher SZA

Edwards et al., AMT, 2018

Including CH_4 emissions in DART/CESM

Tested for CO, in development for CH_4

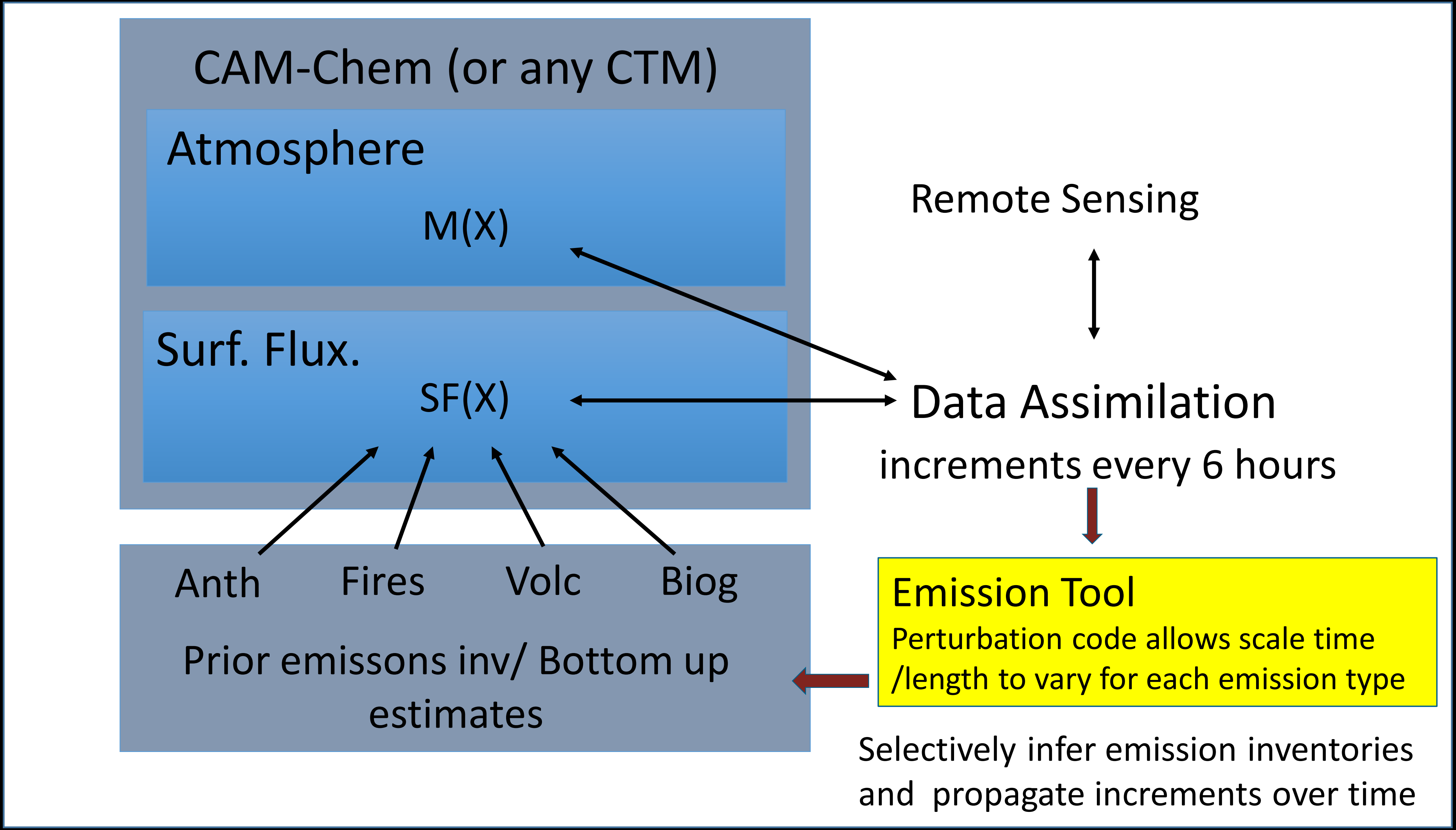

Chemical response to CO assimilation

- MOPITT CO assimilation in CAM-chem in 2002
- Increases CO, particularly in the NH
- Overall improvement against validation
- Resulting decrease in OH; leads to reduced CH_4 oxidation; increases CH_4 lifetime from 8.7 to 9.3 years
- Increase in primary CO emissions is necessary, but also an increase in VOC that oxidize to CO

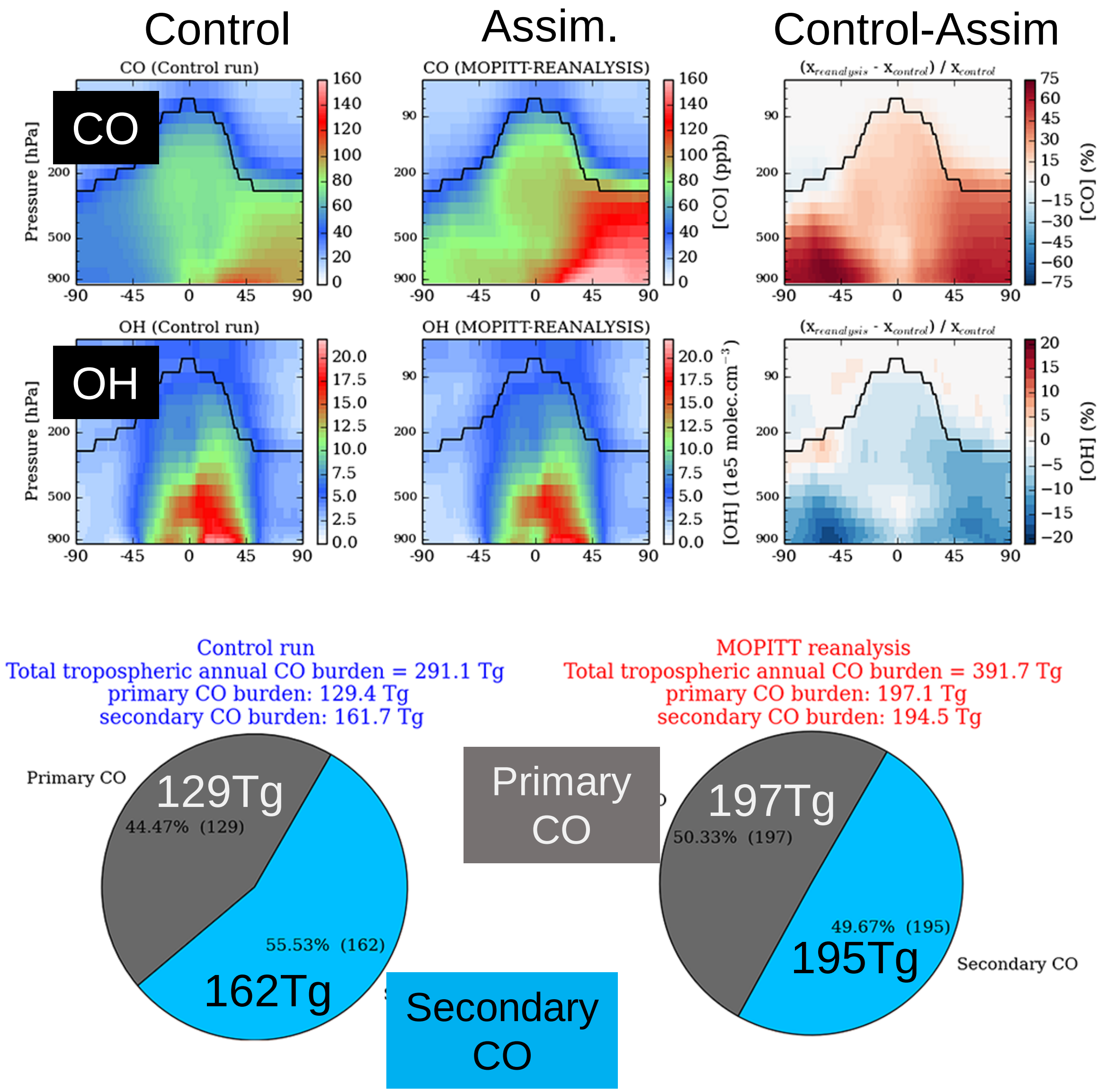

Gaubert et al., JGR, 2016

Decreasing CO abundance reduces methane lifetime

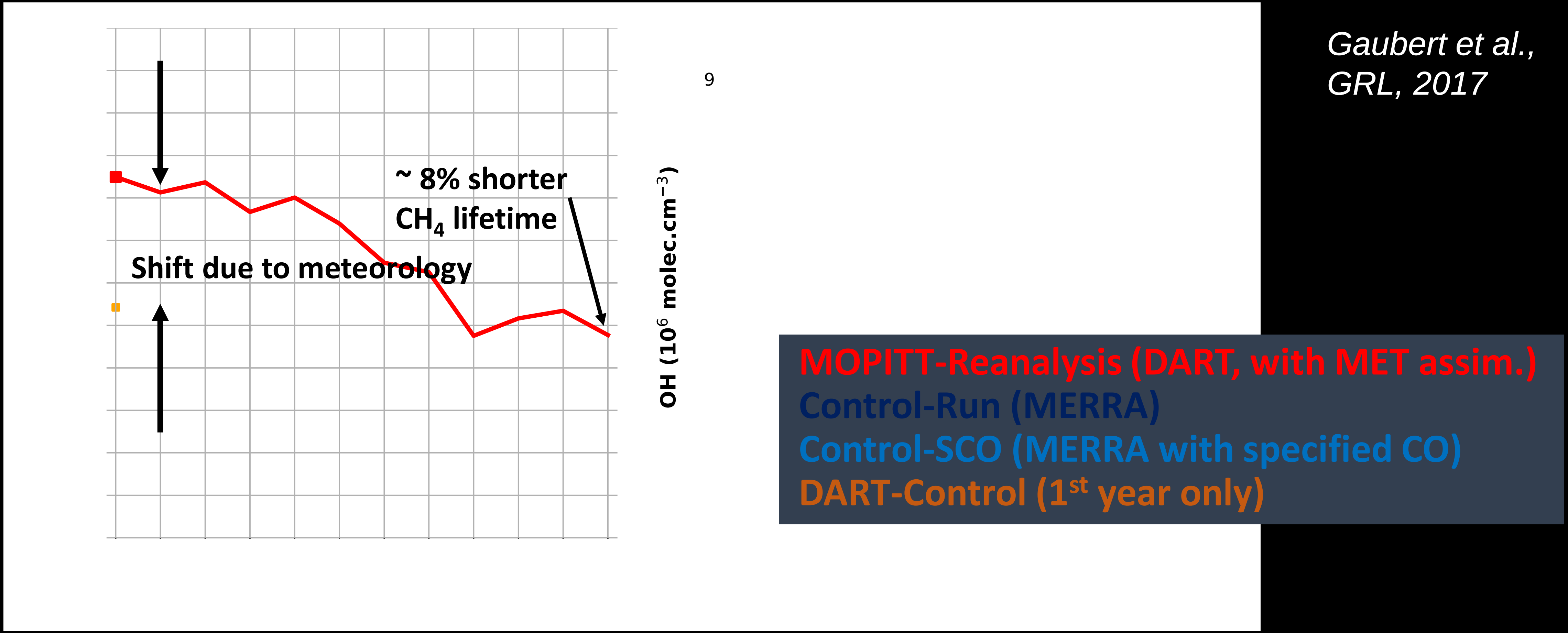

Gaubert et al., GRL, 2017

Although meteorology (MERRA vs. DART assim.) affects the CH_4 lifetime offset, the reduction (slope) in CH_4 lifetime is due mostly to decreasing CO.

Conclusions

- SWIR column CH_4 AKs depend mainly on SZA, satellite ZA and CH_4 amount.
- Only small differences (< 1%) in simulated CH_4 columns are found from using a scene dependent LUT column AK compared to an average AK for column CH_4
  - OSSE results from previous SWIR CH_4 studies do not have large uncertainties from assuming an average AK
- Emission tool for including CH_4 emissions in DART/CESM being developed
- Lifetime of methane has significant dependence on changes in CO through OH
- Decreasing emissions of CO (e.g., BB and China) need to be included in model studies and assessments that aim to attribute changes in methane emissions, abundance, growth rates and lifetime
- Start using TROPOMI CH_4 to see what time/spatial scales are possible for emissions from LEO at 7 km
- Compare these to surface estimates for a well characterized regions (e.g. Greeley with NOAA mobile labs)

The role of wetland emissions within the North America geostationary domain

A. Anthony Bloom, Kevin Bowman, Meemong Lee

Wetlands & the NA CH4 budget

- Wetlands account to ~50% of NA CH_4 budget.
- Major uncertainties on location and extent within and outside NA domain.
- Global constraints on magnitude lead to substantial error correlations between NA and the rest of the world.
- Constraints on NA and global wetlands key to NA GEO mission success.

WetCHARTs mean

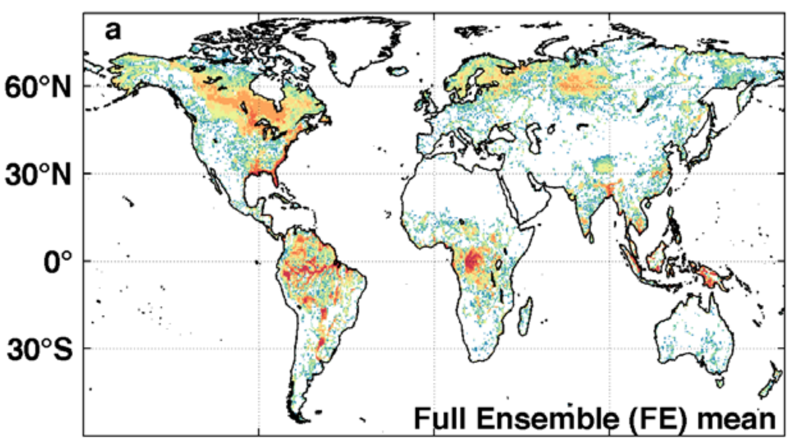

WetCHARTs: uncertainty

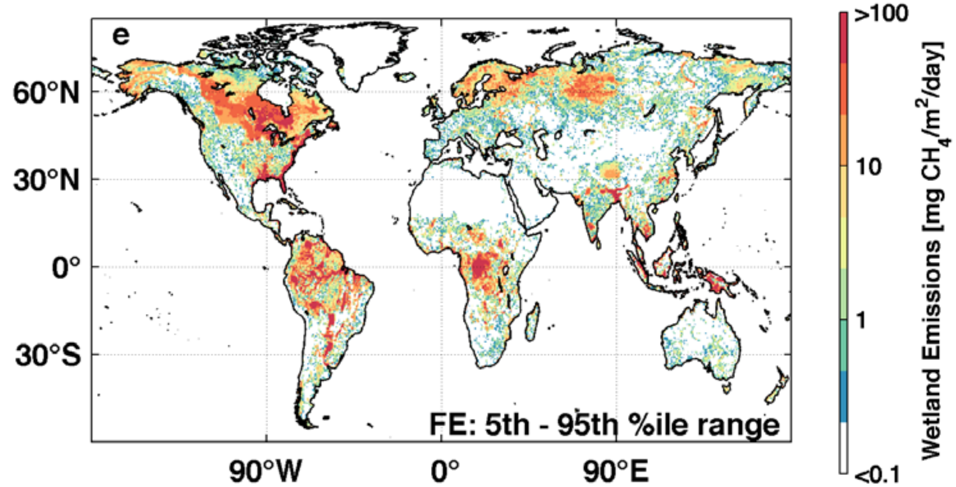

Bloom et al., 2017, GMD

Atmospheric simulations of wetland CH4 within GEO-CAPE domain

January & July mean XCH4 concentrations

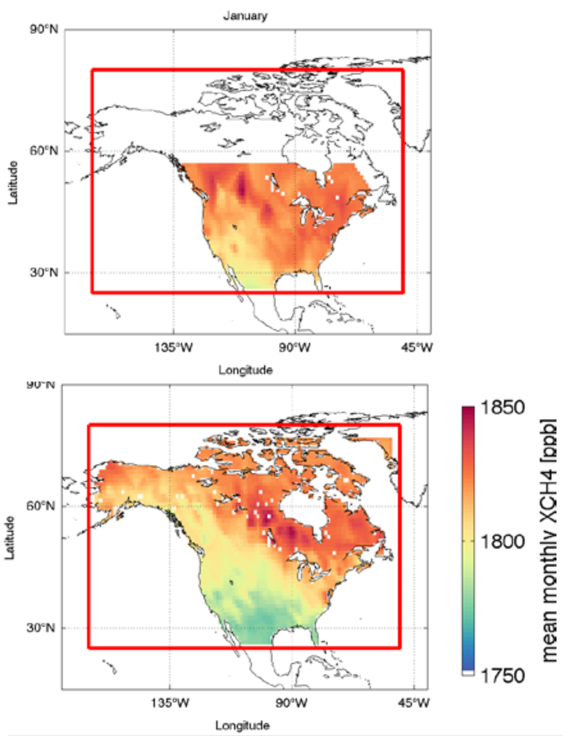

Uncertainty: based on 3 wetland emission scenarios. Range comparable to WETCHIMP model range

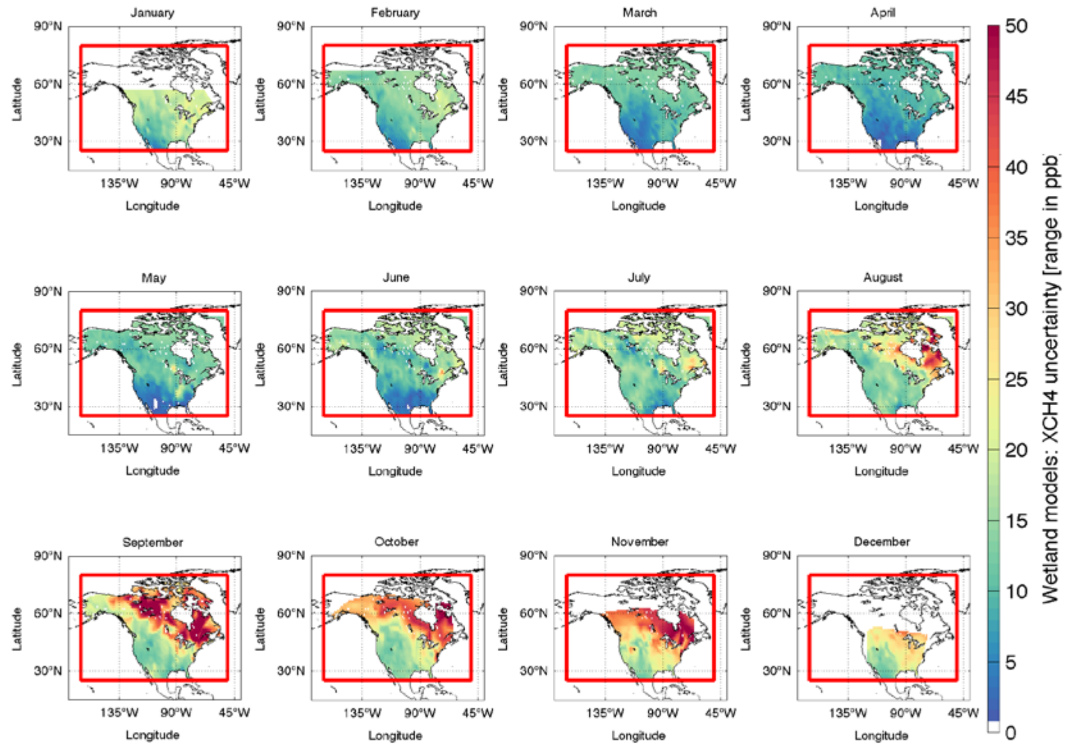

1. GEO-CAPE XCH_4 observations can differentiate between summer-time (July-October) enhancements due to wetland CH4 emission scenarios (provided a 1.1% - approx. 20ppb - observational precision; Wecht et al., 2014).
2. Large uncertainty (comparable to typical XCH4 spatial variability) due to uncertainty in the magnitude and timing of wetland CH4 emissions.

GEO-CAPE North America Wetland OSSE

Objective: *quantify GEO-CAPE CH_4 measurement constraints on NA wetland CH_4 emissions.*

1. **Improving estimates of wetland CH_4 emissions at ~300km- 500km resolution is necessary to:**
   - **capture main continental wetland structures, and**
   - **Resolve the first order inter-model differences.**

WETCHIMP model ensemble: mean wetland CH_4 emissions

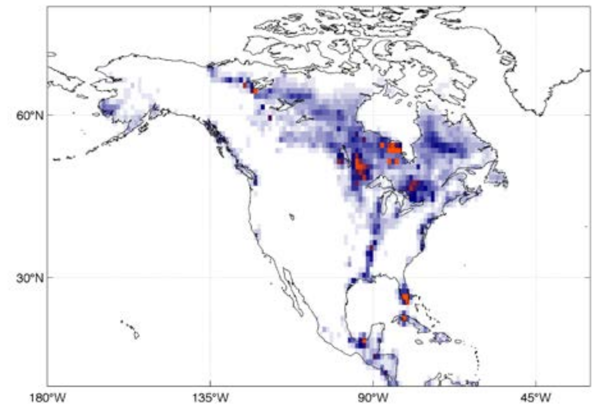

WETCHIMP model spatial correlations

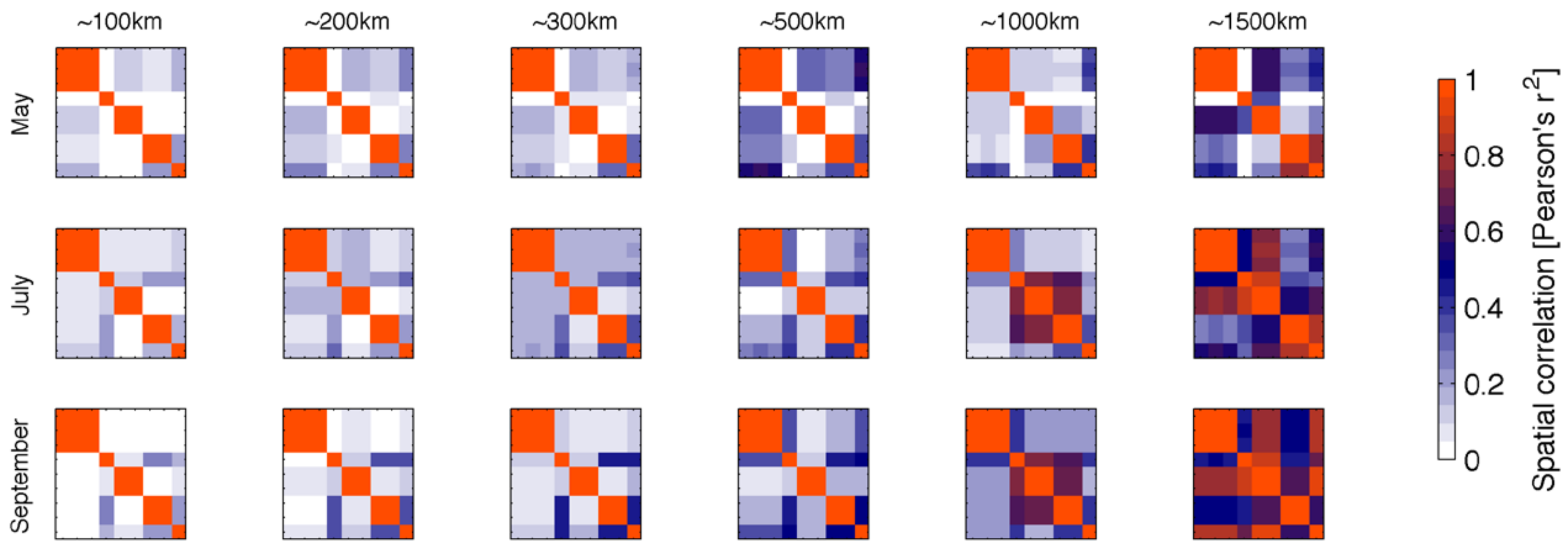

Satellite-constrained wetland CH_4 flux uncertainty

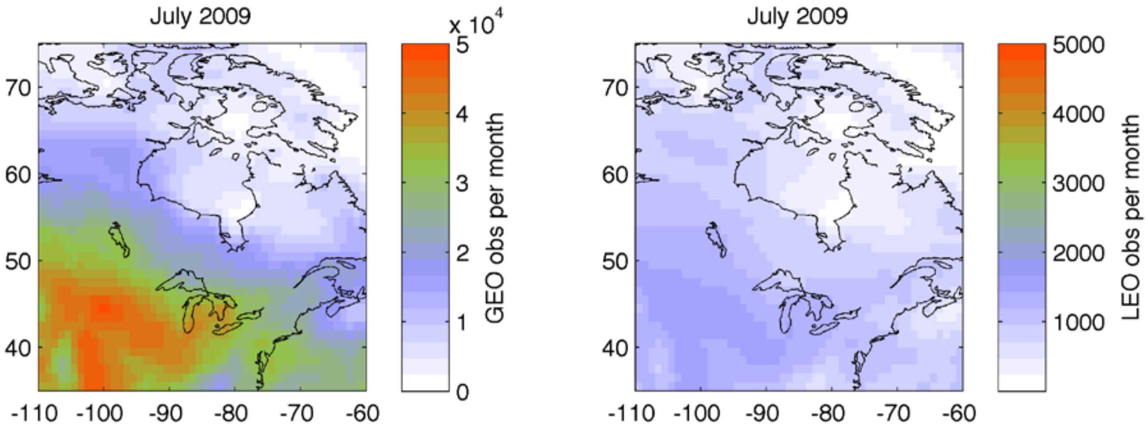

MODIS cloud-cover

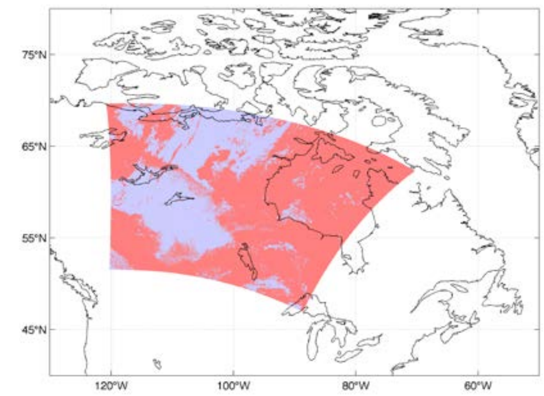

Step 1. *Number of GEOCAPE and TROPOMI observations in July 2009 using MODIS cloud cover, ERA-interim cloud cover & sunshine hours.*

Step 2. *Construction of mock atmospheric operator using GEOS-Chem adjoint.*

Step 3. *Wetland CH_4 flux uncertainty, based on Monte Carlo perturbation of GEO-CAPE and TROPOMI concentrations using Wecht et al., 2014 observation uncertainty.*

(Analysis described by Bloom et al., 2016).

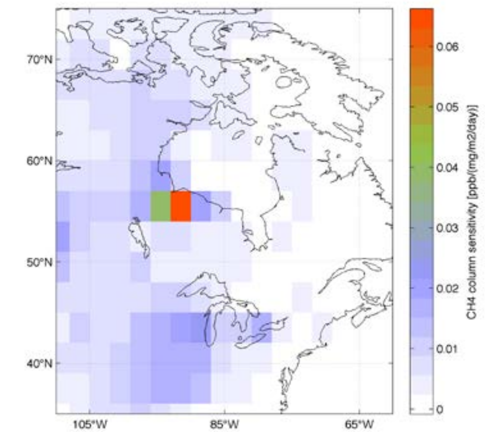

Example CH_4 column influence function: derived using GOSAT averaging kernel and GEOS-Chem CH_4 adjoint.

MODIS cloud cover

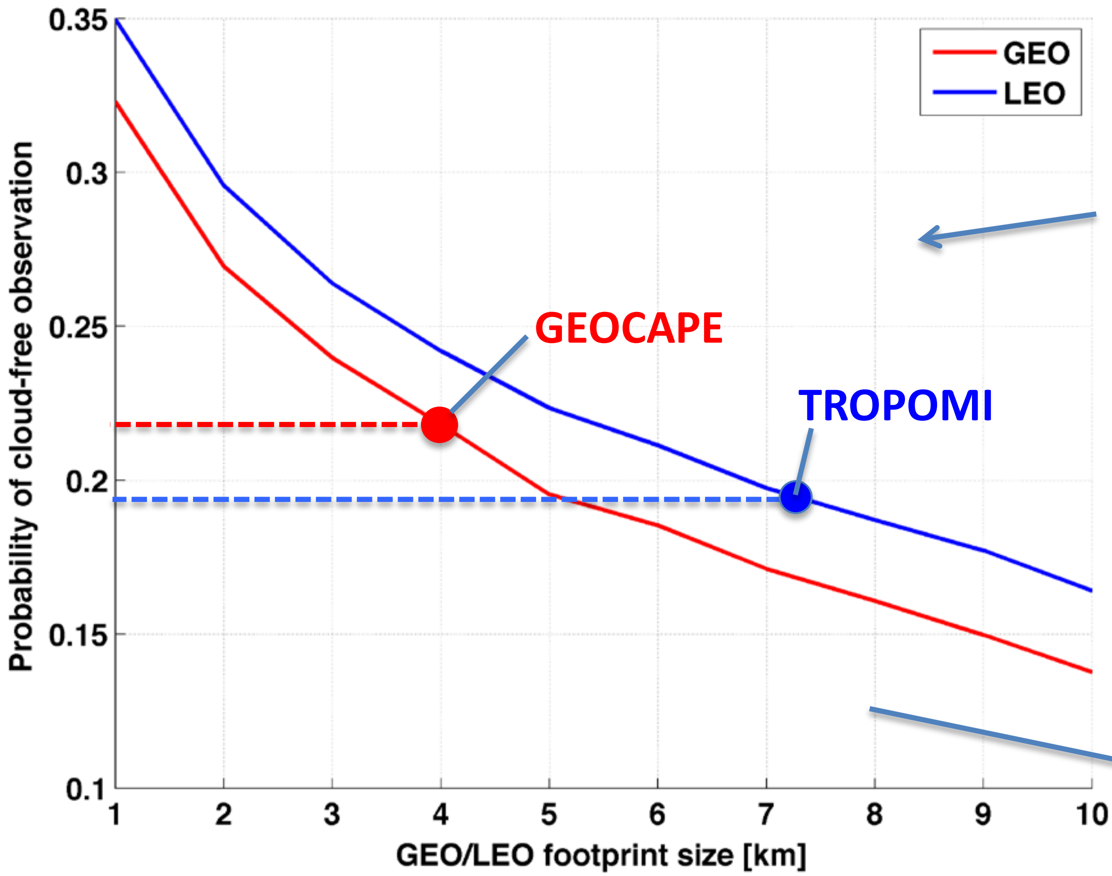

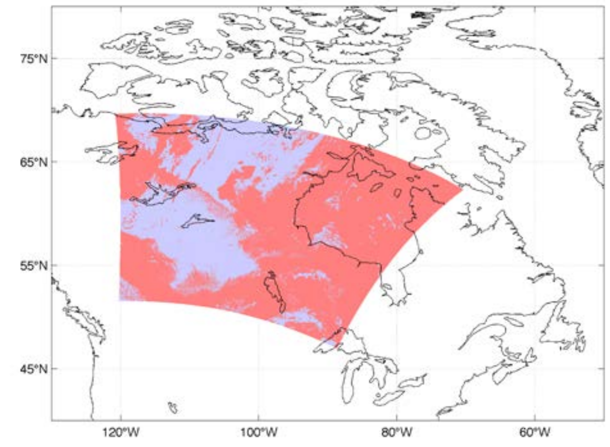

Example: 1km x 1km MODIS cloud cover

Cloud-free domain ≠ Cloud-free observations

- GEOCAPE: smaller pixel size increases cloud-free observation yield (despite ~60° angle from nadir)
- We use MODIS cloud cover statistics to derive ERA-interim cloud-free cover domain for GEOCAPE (0.6) and TROPOMI (0.5)

GEO-CAPE wetland CH_4 OSSE: example

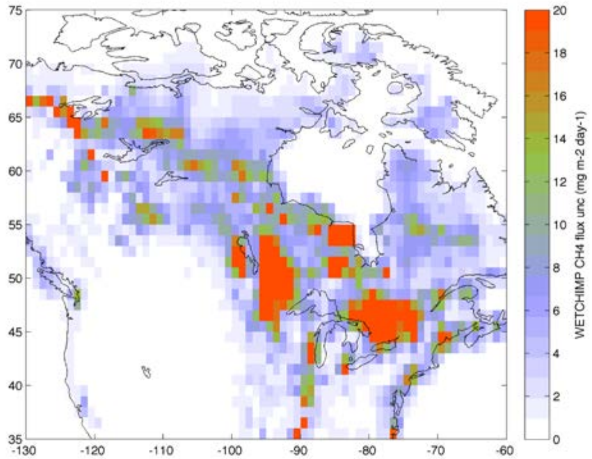

July WETCHIMP uncertainty

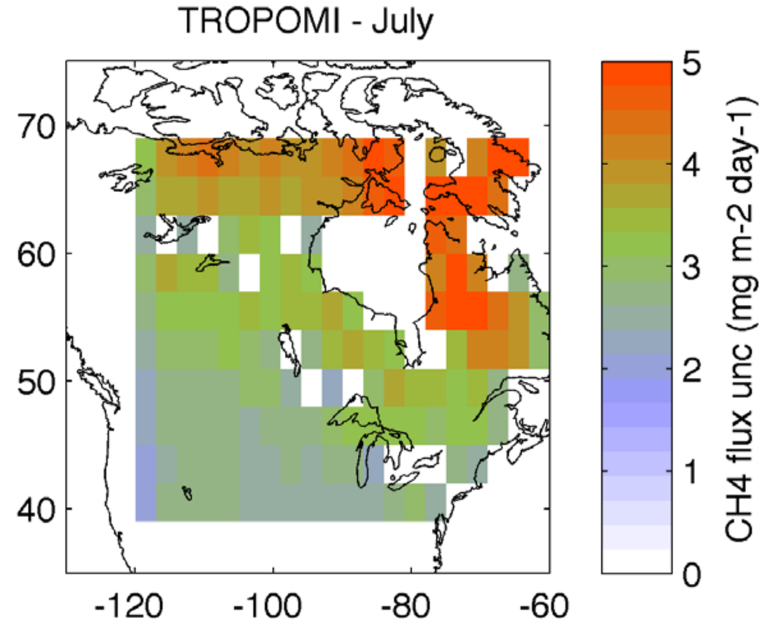

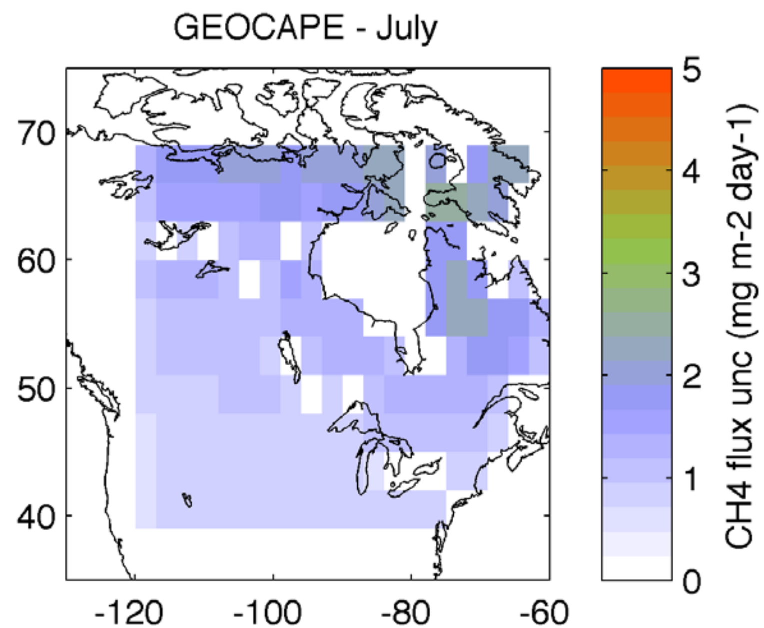

1. **Example, July 2009: GEO-CAPE observations indicate factor ~2 improvement (relative to TROPOMI) in ~300km CH4 flux estimates in major NA wetland region.**

2. **Based on preliminary simulation of GEO-CAPE retrieved flux uncertainty, GEO-CAPE measurements will provide substantial constraints on WETCHIMP wetland model CH4 uncertainties.**

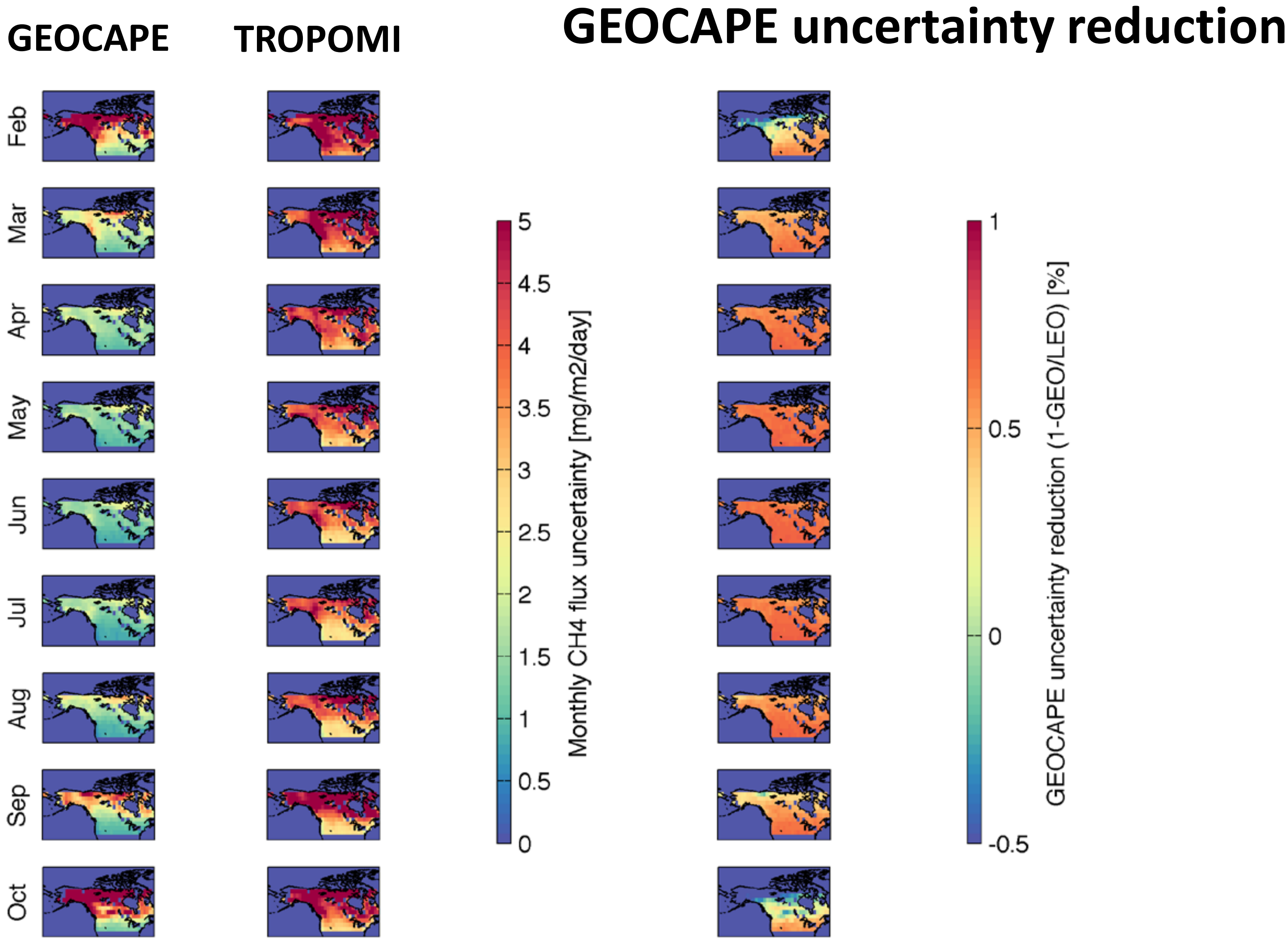

1. GEOCAPE yields 60% uncertainty reduction (relative to TROPOMI) over NA wetlands
2. GEOCAPE advantage is largest in summer (coincides with largest CH_4 emissions).
3. Fewer sunlight hours in shoulder seasons reduce the relative advantage of GEOCAPE.

Satellite-retrieved and model ensemble CH4 flux uncertainty

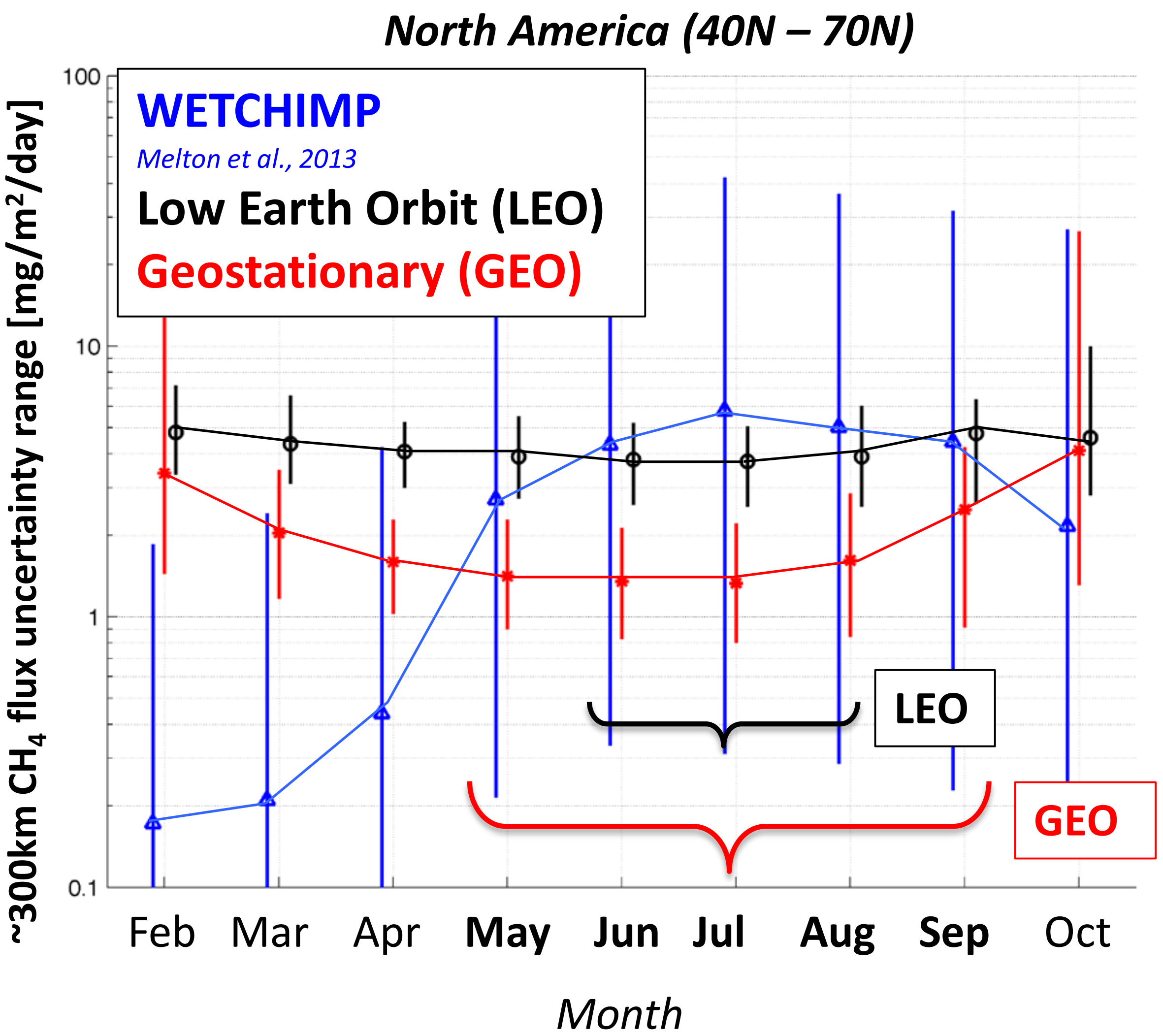

1. **Low Earth Orbit** can improve median WETCHIMP CH4 uncertainty for 3-month period (Jun – Aug).
2. **Geostationary:** can improve median WETCHIMP CH4 uncertainty for 5-month period (May – Sep).
3. **Geostationary:** can potentially constrain early season CH4 fluxes in high-emission wetland regions.

Biogeochemical constraints on wetland CH4 emissions: lessons learned from Amazon OSSE

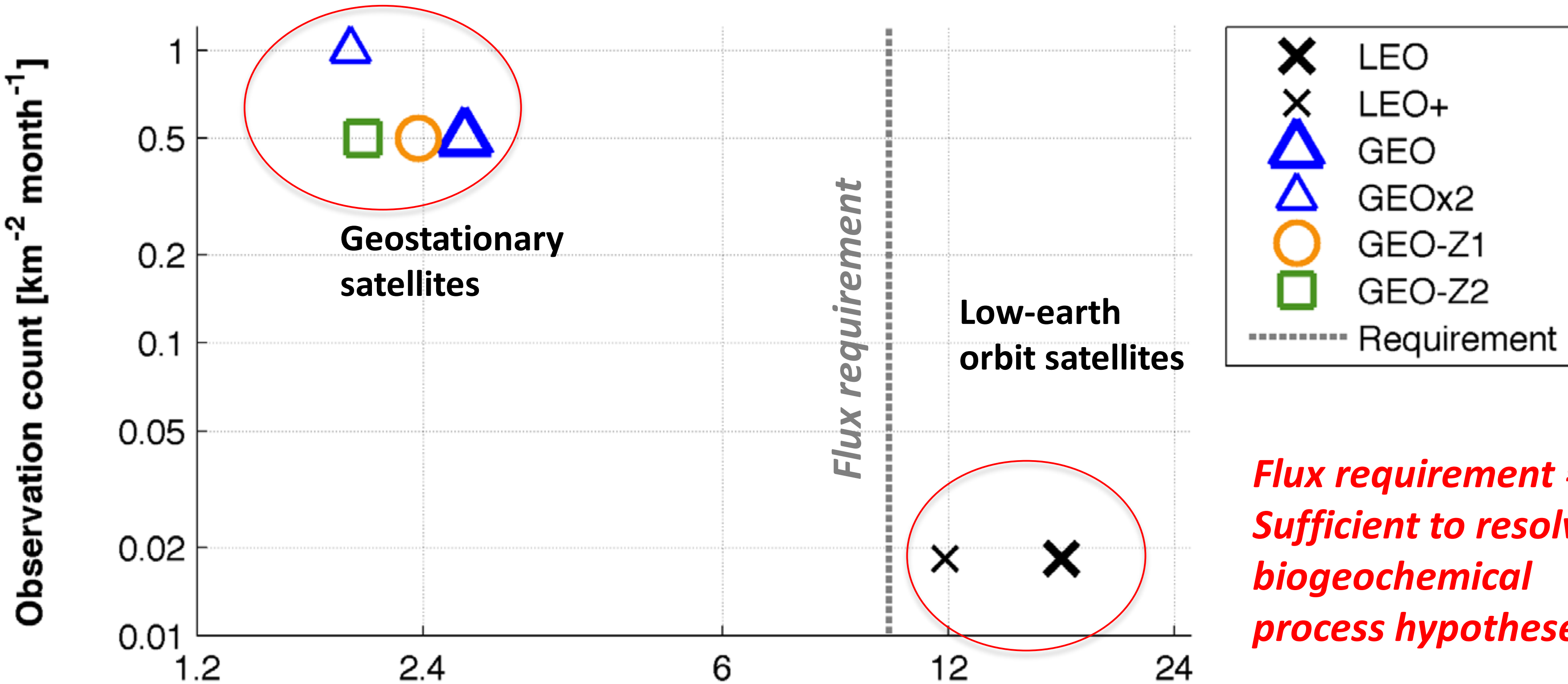

Flux requirement = Sufficient to resolve biogeochemical process hypotheses

Bloom et al., 2016 (ACP)

FLUX UNCERTAINY [mg CH_4/m2/day]

- **Geostationary OSs can resolve CH4 fluxes at a sufficient resolution to distinguish between key biogeochemical process hypotheses**
- **Biogeochemical insights crucial for understanding seasonal and year-to-year evolution of NA CH4 budget**

Conclusions

- Wetlands are a central component of the NA domain and its boundary conditions.
- Reducing uncertainties in magnitude and timing of wetlands key to deciphering the NA budget.
- Geostationary mission will provide substantial uncertainty reductions on wetland model CH_4 emissions.
- Based on Amazon OSSE, geostationary mission will likely resolve fluxes at sufficient resolution to test biogeochemical process hypotheses, which are central to understanding the evolution of the NA CH_4 budget.

Spare slides

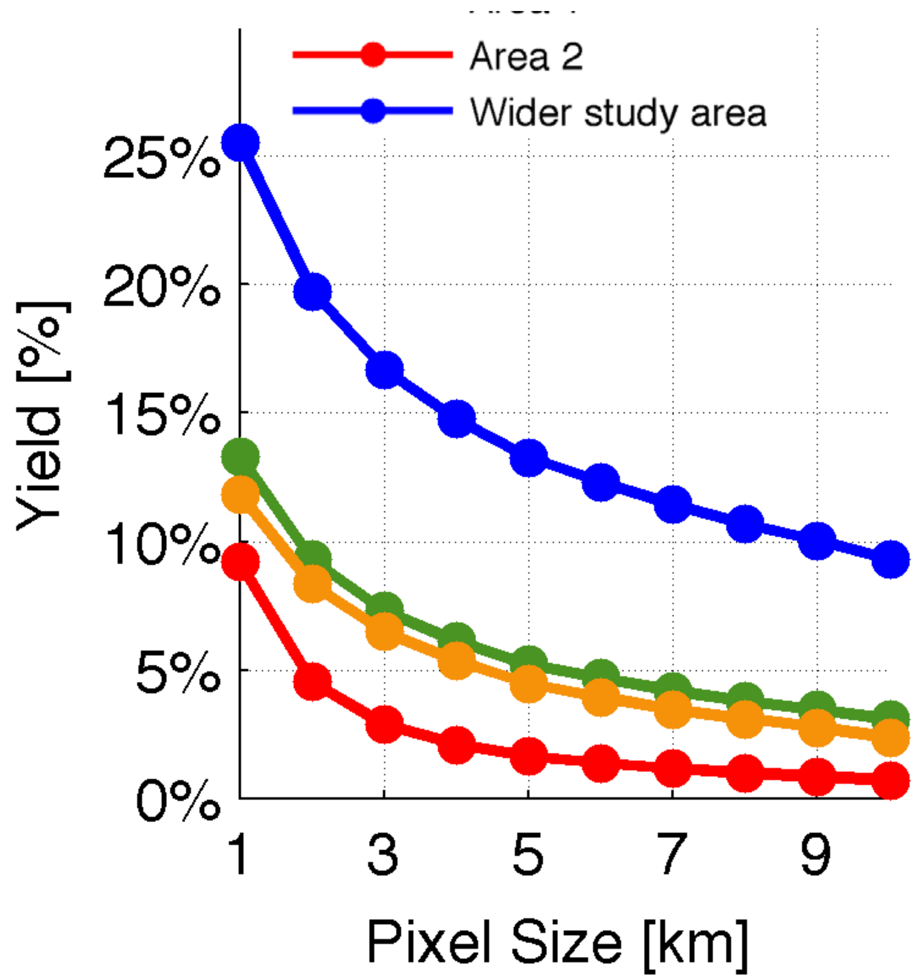

Bloom et al., 2016 (ACP)

0%

MODIS mean monthly cloud cover

Cloud cover: MODIS imagery was used to assess the role of pixel size in the abundance and spatial distribution of cloud-free CH4 observations.

Part 2: what observing system is needed to reduce biogeochemical process uncertainty?

Amazon CH_4 emissions as a case study

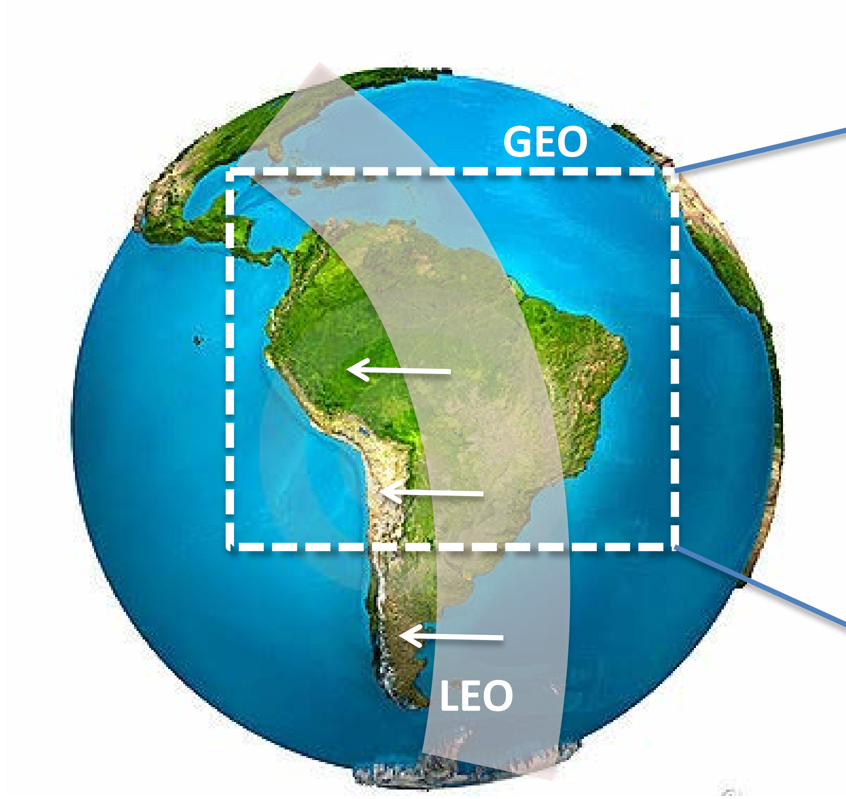

Step 3. Define CH_4 observation system requirements — *Atmospheric concentrations*

↑

Step 2. Define CH_4 flux requirements — *Wetland fluxes*

↑

Step 1. Characterize wetland CH_4 process controls — *Wetland processes*

Bloom et al., 2016 (ACP)

Observing system simulation experiment (OSSE)

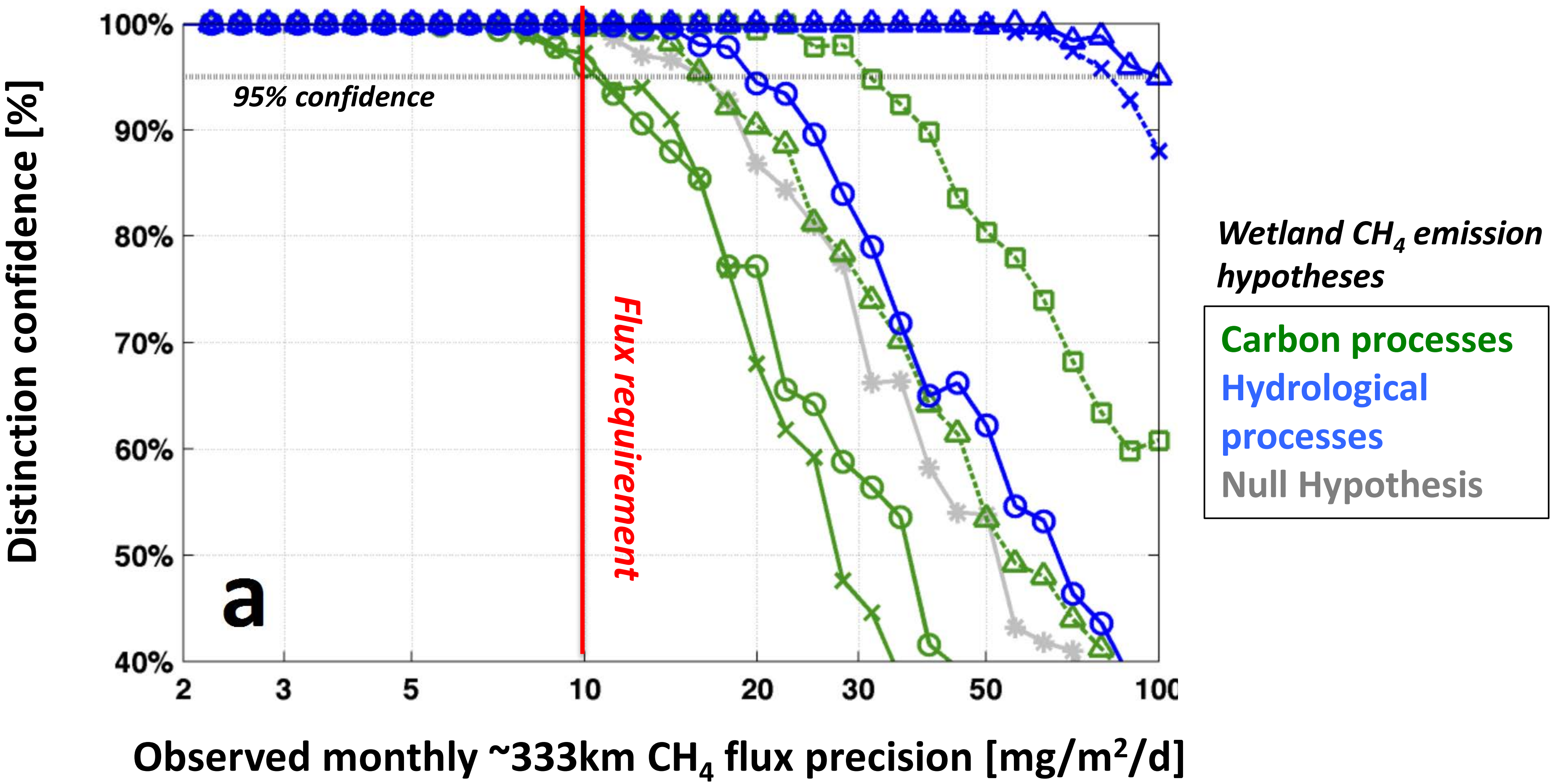

Bloom et al., 2016 (ACP)

Top-down CH_4 flux requirement: *333km, monthly, 10 mg CH_4 m^{-2} day^{-1}*

Simulated Geostationary CH_4, CO_2, CO and Aerosol Measurements Testbed: California Laboratory for Atmospheric Remote Sensing

Liyin He, Clare Wong[1], Thomas Pongetti[1], Qiong Zhang[2], Zhao-Cheng Zeng[2], Vijay Natraj[1], Sally Newman[2], Yuk L. Yung[2], Kevin Gurney[3], Stanley P. Sander[1]

[1]NASA Jet Propulsion Laboratory, California Institute of Technology
[2]Division of Geological and Planetary Sciences, California Institute of Technology
[3]School of Life Sciences, Arizona State University

Objectives for GEO-CAPE pre-phase A studies

1. Using an observing system for trace gases that emulates a spectrometer in geostationary orbit, obtain spatially and temporally resolved fluxes of trace gases including CH_4, CO_2 and CO from column abundance measurements.

2. Assess the impact of confounding variables including high and low clouds and aerosols, topographic relief, and surface albedo variations

3. Use these results to refine the measurement and instrument requirements for instruments on future missions.

4. Continue to develop the technology for future imaging Fourier transform spectrometers such as PanFTS.

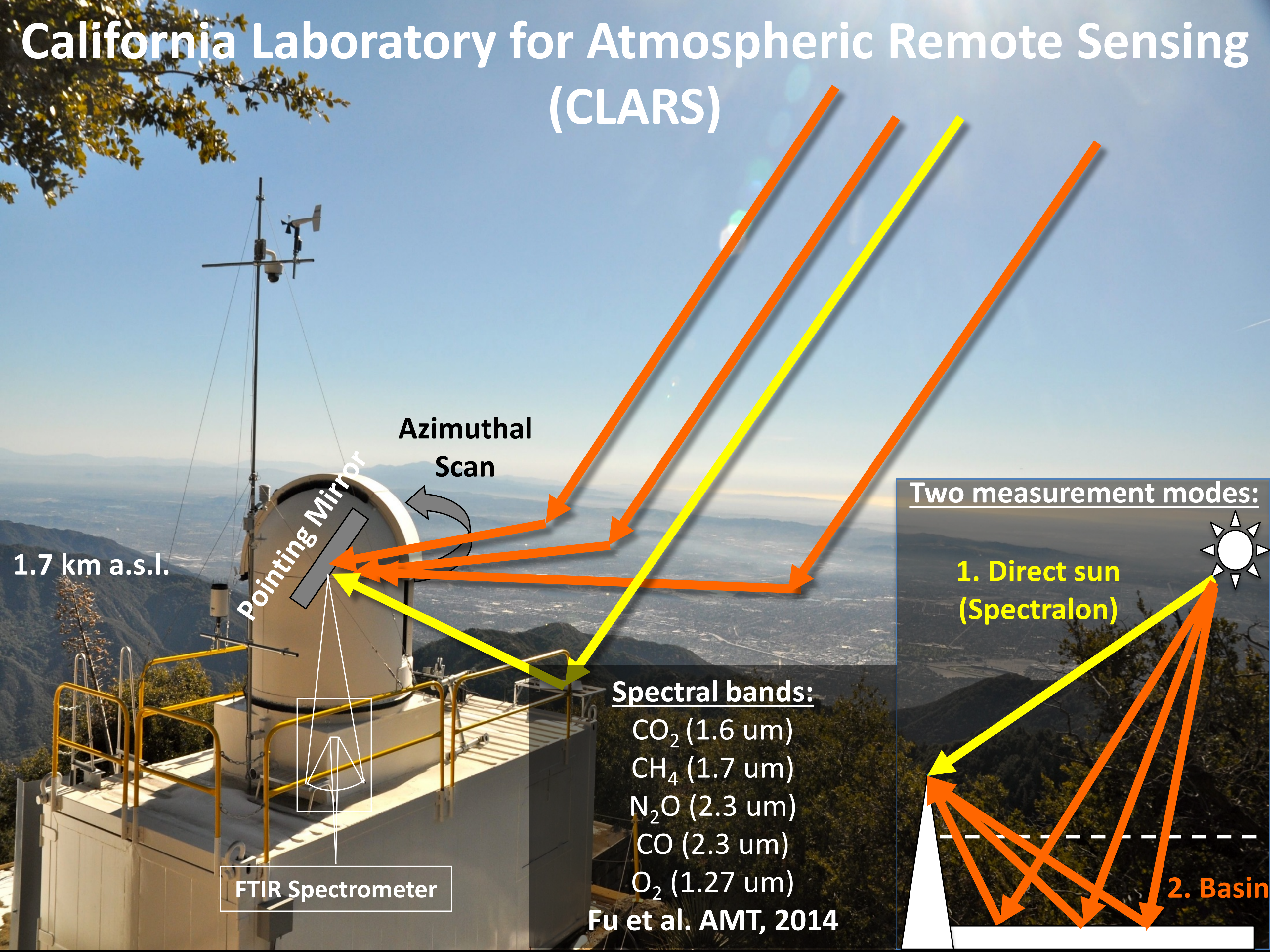
California Laboratory for Atmospheric Remote Sensing
(CLARS)
Azimuthal
Scan
Pointing Mirror
1.7 km a.s.l.
FTIR Spectrometer
Spectral bands:
CO_2 (1.6 um)
CH_4 (1.7 um)
N_2O (2.3 um)
CO (2.3 um)
O_2 (1.27 um)
Fu et al. AMT, 2014
Two measurement modes:
1. Direct sun
(Spectralon)
2. Basin

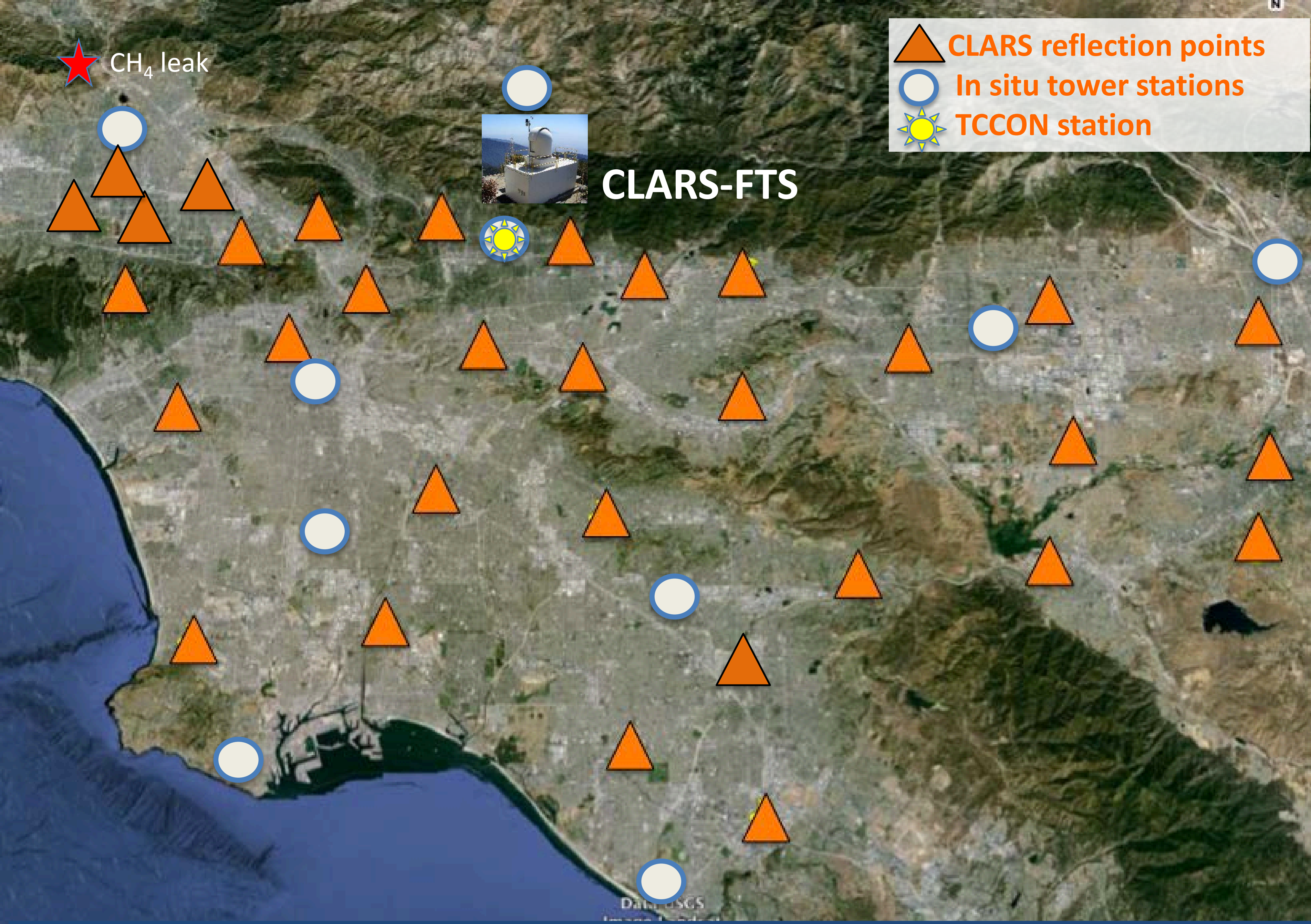

4-8 mapping cycles/day depending on season, clouds and aerosols

Diurnal variations of Direct Sun & Basin XGAS

- Direct sun XGAS diurnal variability is small as expected
- Basin XGAS shows strong diurnal variation due to basin emissions.
- CLARS basin XGAS is strongly weighted to the boundary layer due to large VZA

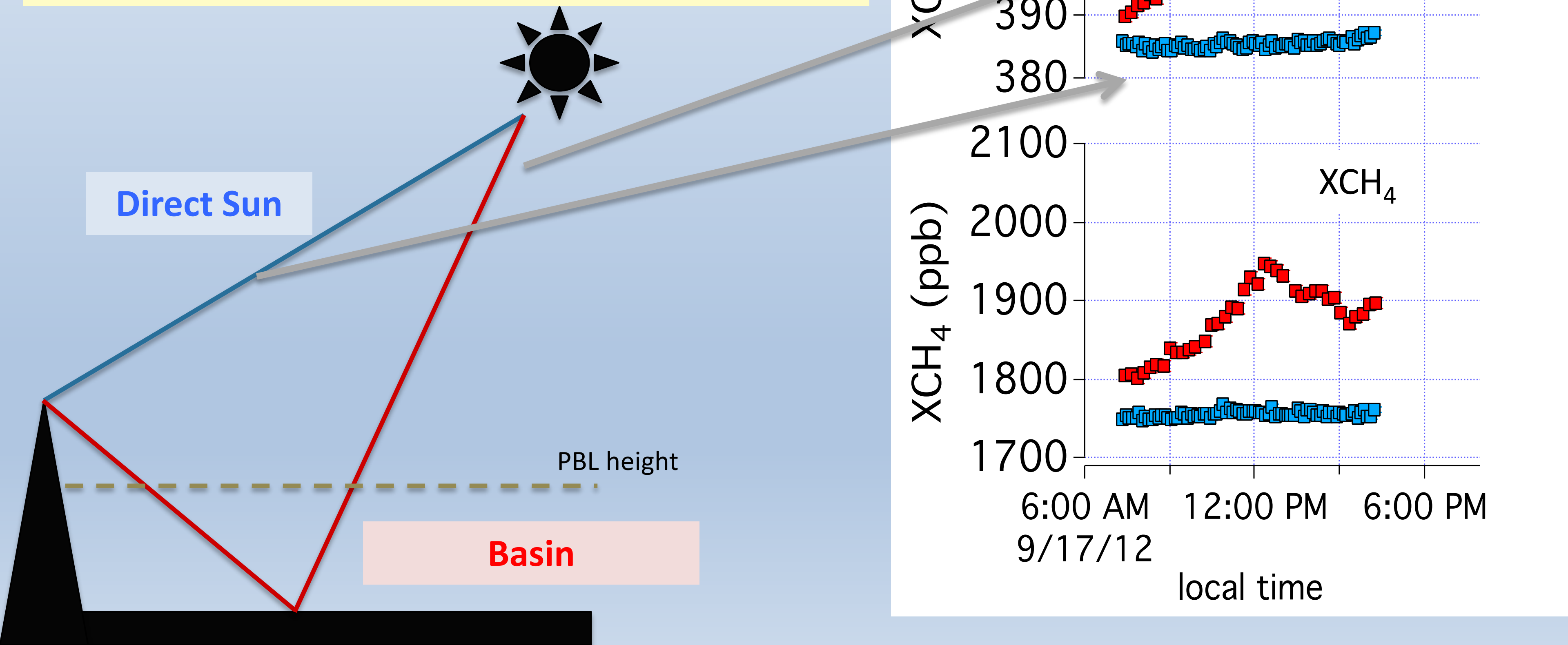

Correlation Between XCH_4 and XCO_2 Excess

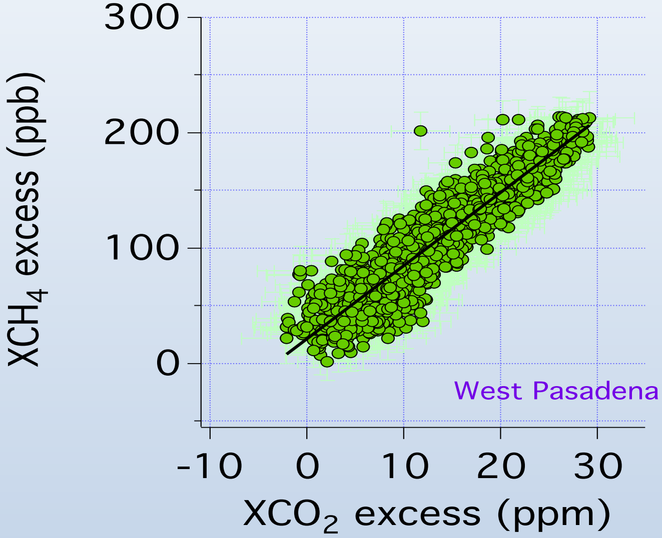

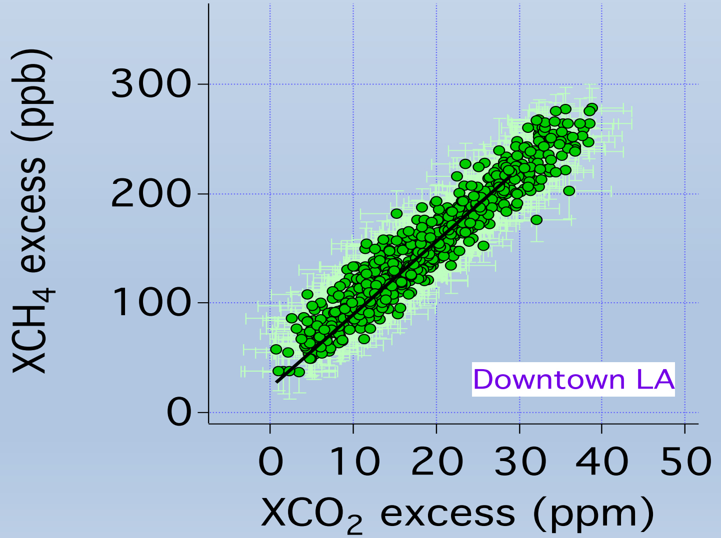

Period: September 2011 – October 2013

- Tight correlations between XCO_2 and XCH_4 excess are observed at every reflection point even though they are emitted by different sources – why?

- Both species are chemically inert, so the variabilities of both CO_2 and CH_4 are controlled primarily by local emissions and advection.

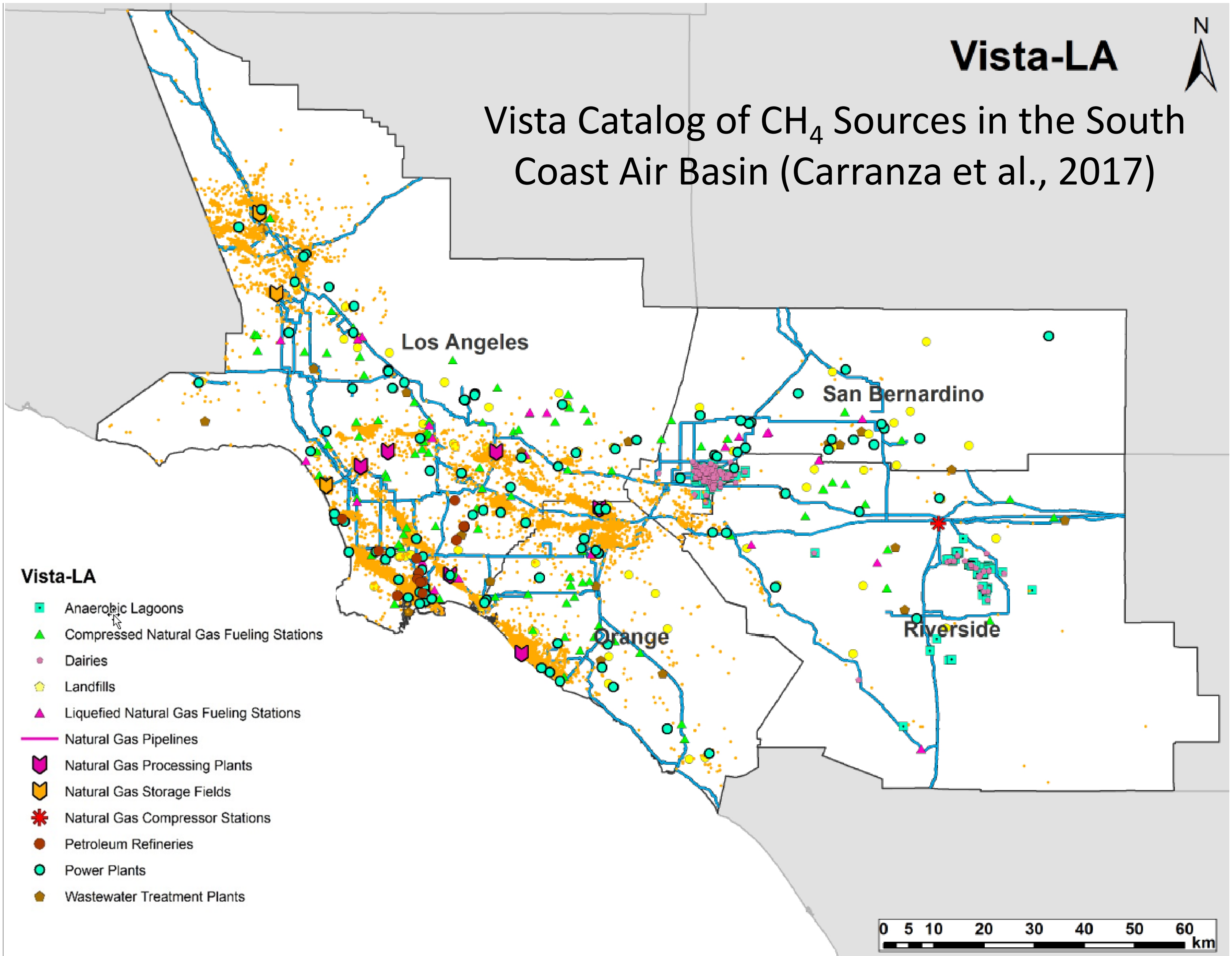

Vista-LA
N
Vista Catalog of CH_4 Sources in the South Coast Air Basin (Carranza et al., 2017)
Los Angeles
San Bernardino
Orange
Riverside
Vista-LA
Anaerobic Lagoons
Compressed Natural Gas Fueling Stations
Dairies
Landfills
Liquefied Natural Gas Fueling Stations
Natural Gas Pipelines
Natural Gas Processing Plants
Natural Gas Storage Fields
Natural Gas Compressor Stations
Petroleum Refineries
Power Plants
Wastewater Treatment Plants
0 5 10 20 30 40 50 60
km

Map of XCH_4:XCO_2 Excess Ratio

- Scholl Canyon landfill
- NG pipeline

- Puente Hills landfill
- Fracking sites

Dairy farms

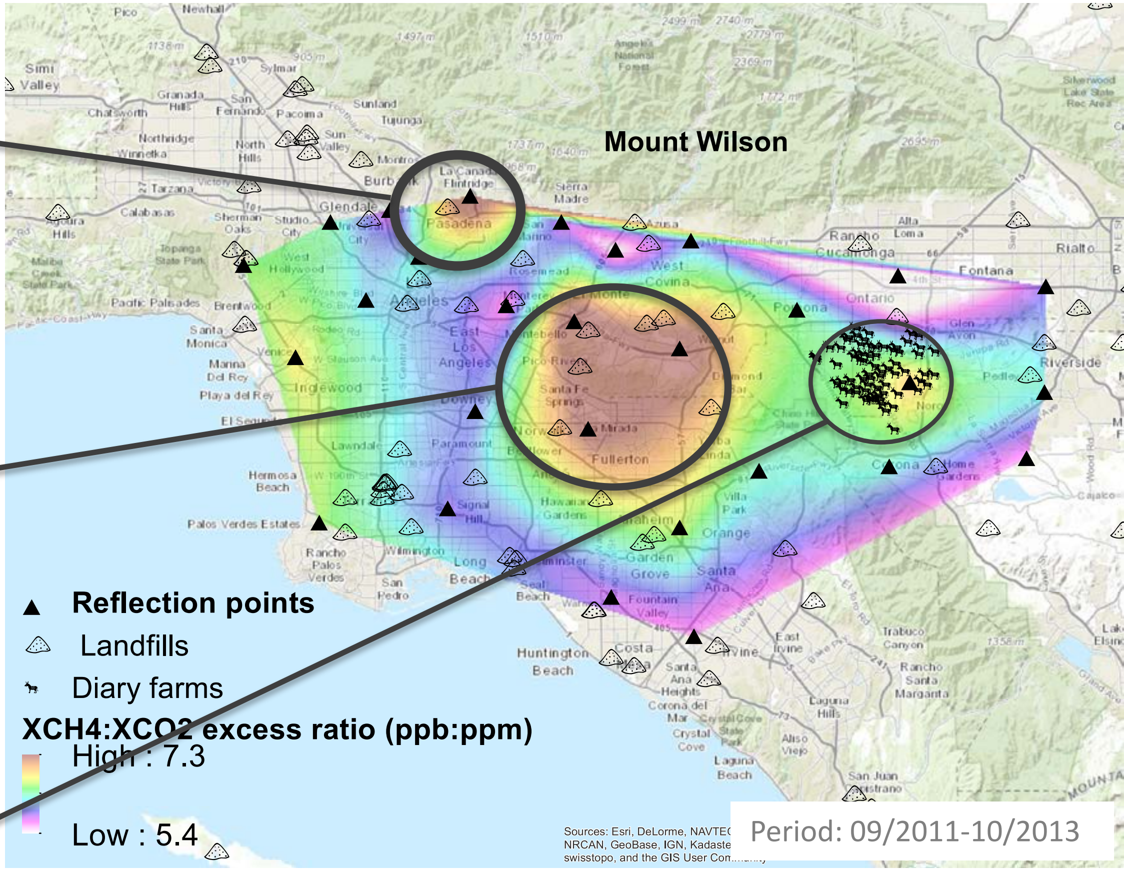

*Attribution of CH_4 hot spots to specific sources is not feasible. Other methods are required, e.g. in situ measurements, isotopic fractionation

Basin-wide CH_4 emissions inventory

Using CLARS FTS XCH_4:XCO_2 excess ratio measurements, basin-wide CH_4 emissions are given by:

$$E_{CH_4}|_{top-down} = E_{CO_2}|_{bottom-up} \times \frac{XCH_4}{XCO_2}|_{slope} \times \frac{MW_{CH_4}}{MW_{CO_2}}$$

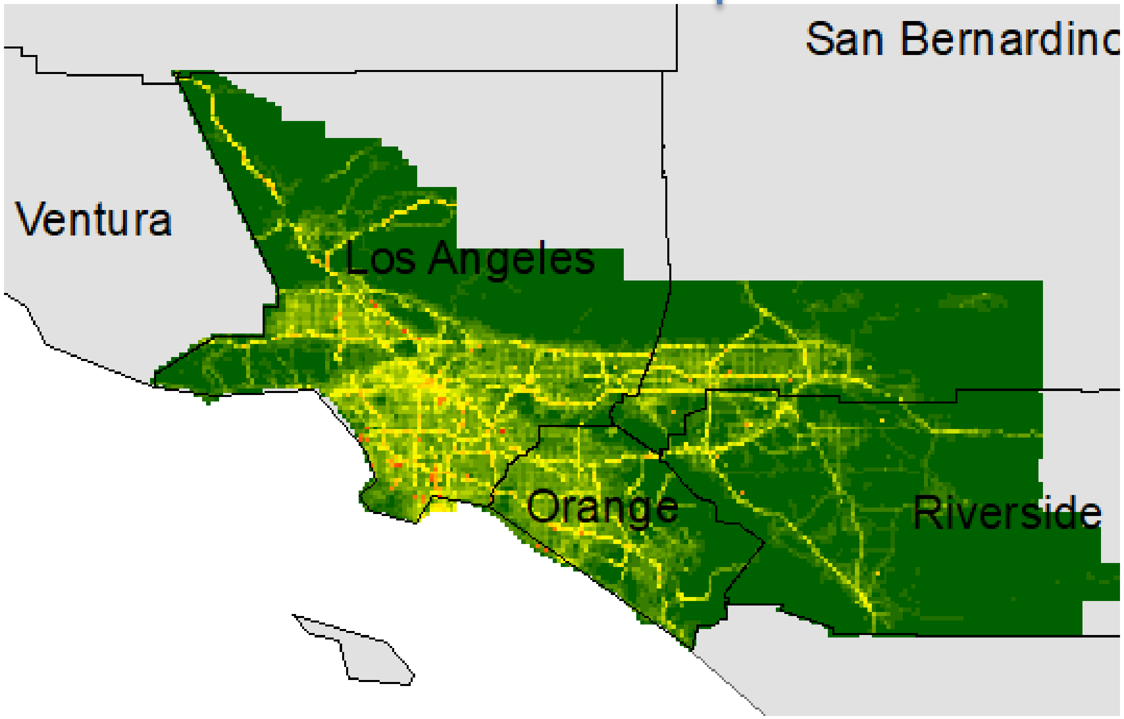

Bottom-up CO_2 emissions from the Hestia v2.4 inventory in the South Coast Air Basin (Gurney et al.):

- Building scale
- Hourly

CLARS-FTS Monthly Methane Emissions in the LA Basin

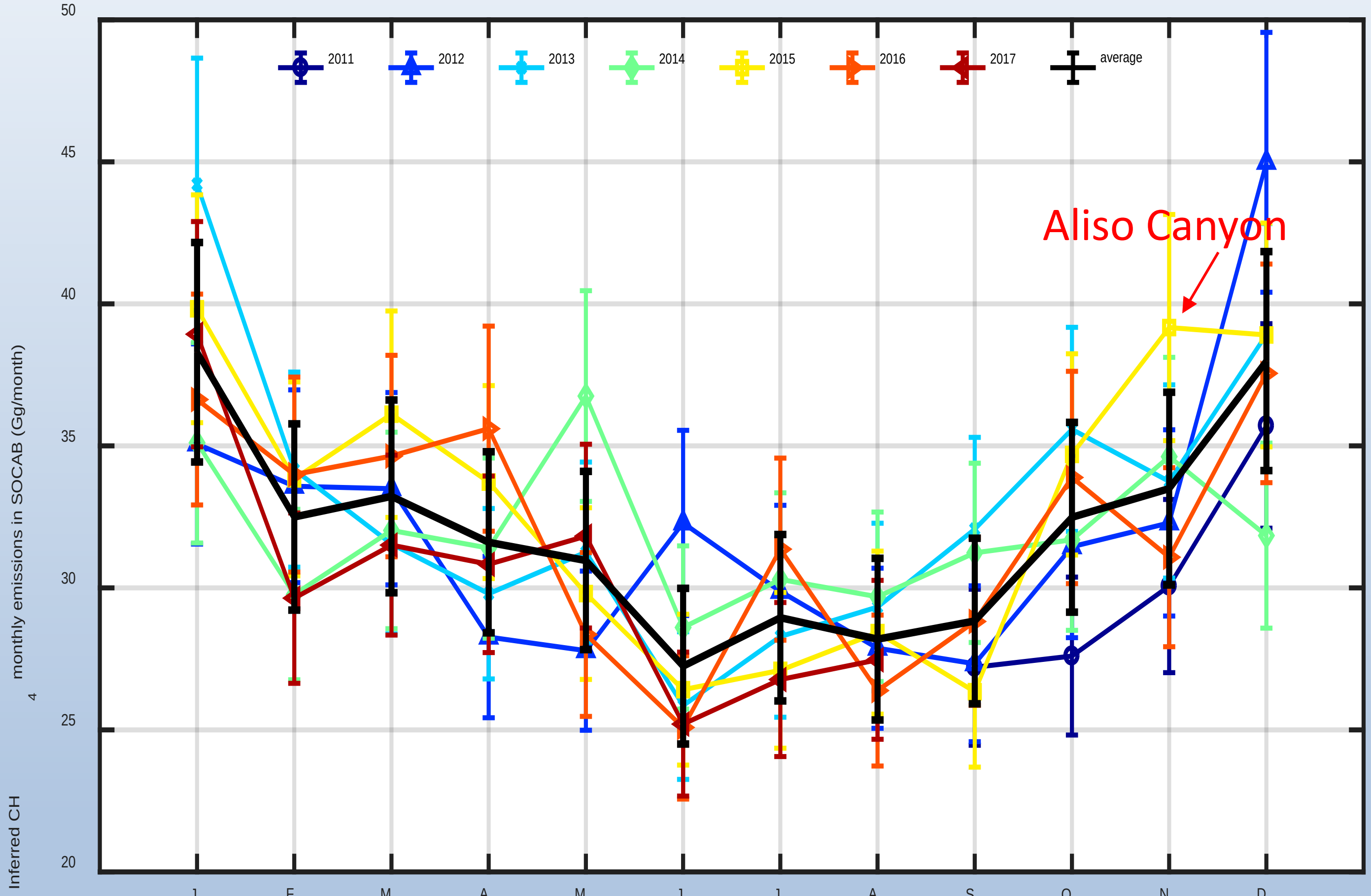

Annual monthly pattern of CH4 emissions is highly repeatable with large winter maximum

CLARS-FTS Monthly Methane Emissions in the LA Basin

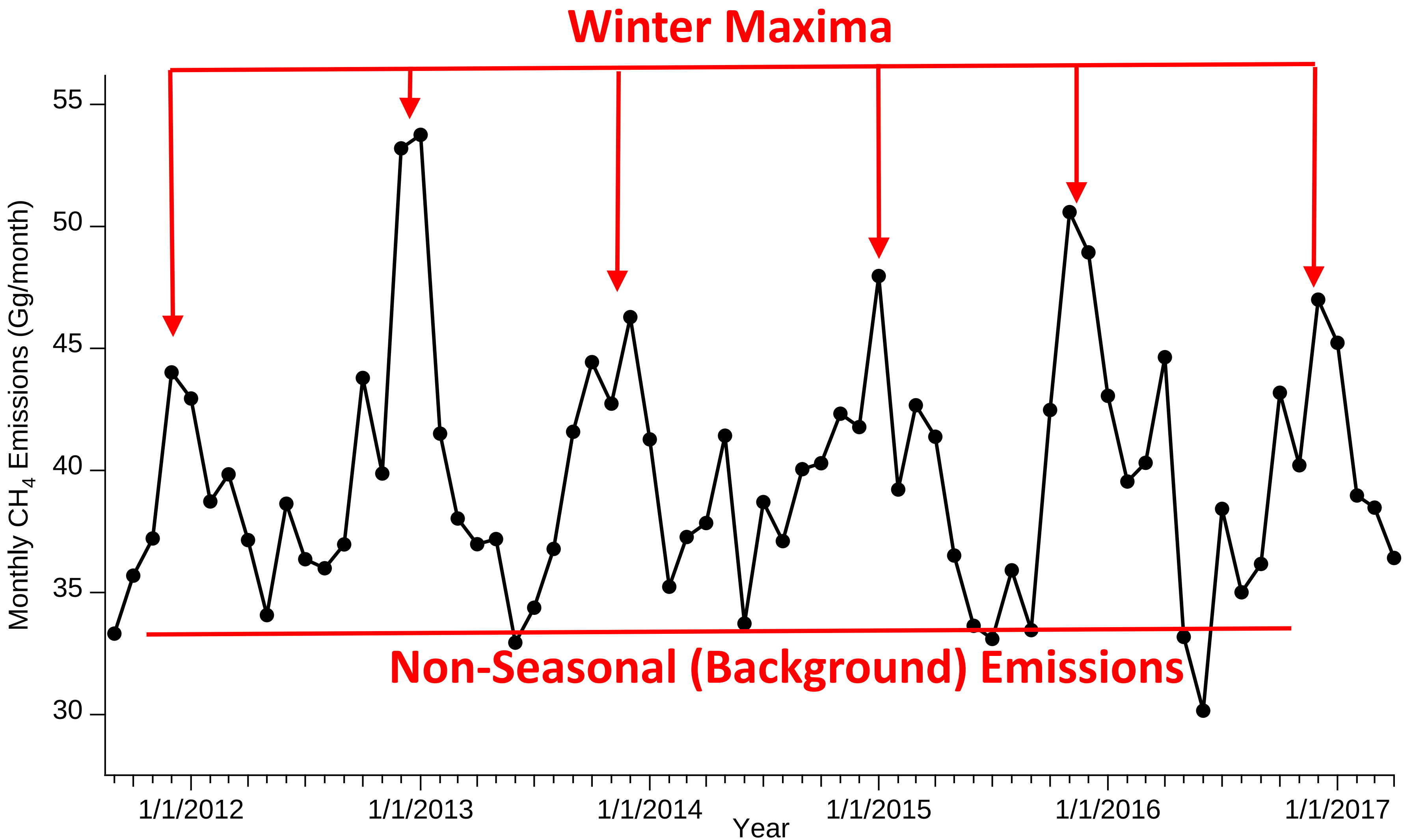

- **CLARS-FTS data reveal prominent annual peaks in CH4 emissions as well as non-seasonal background emissions**

Annual CH_4 Emissions Estimates in the past 10 years in Los Angeles

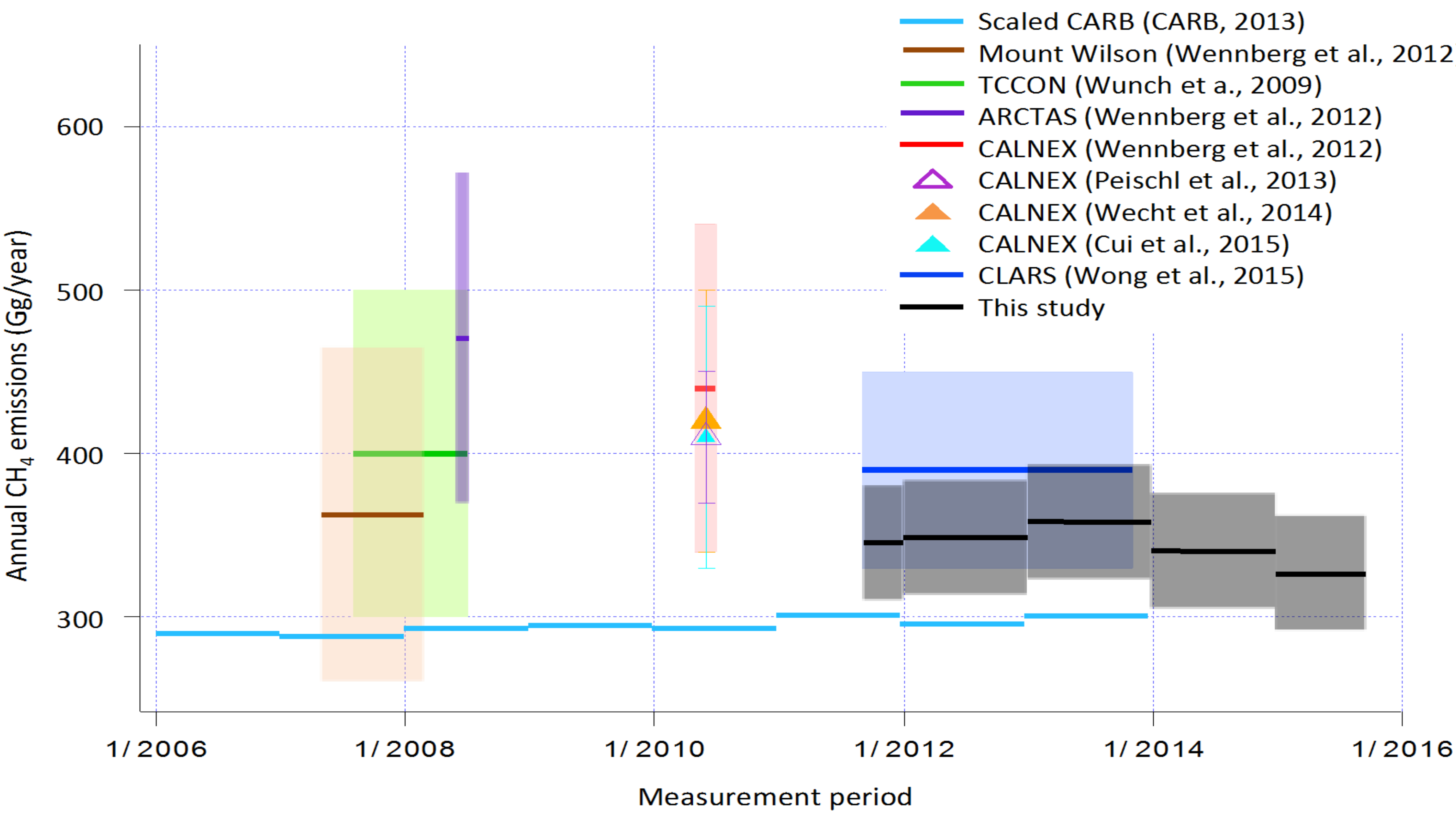

- CLARS observations are consistent with previous estimates.
- Scaled CARB CH_4 emissions from 2011 to 2013 were 2-31% lower than our estimates.

Tracking CH4 Transport Over the LA Basin from an Episodic Release: Aliso Canyon Natural Gas Storage Well Blowout

SoCal Gas

LA Daily News

Repairing Porter Ranch leaking gas well may take 4 months

LA Daily News

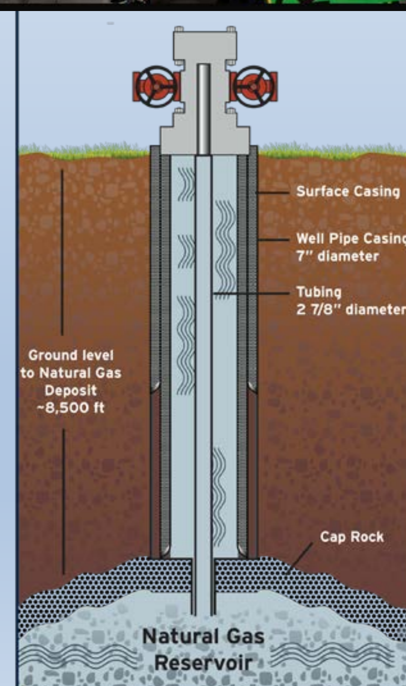

SoCal Gas

- NG leak is due to a broken pipe below the surface.
- 4 months were required to drill a relief well to cap the leaking well with concrete

Snapshot (2 p.m.) images of XCH_4/XCO_2 from Aliso Canyon

Leak started on 10/23 according to SoCal Gas

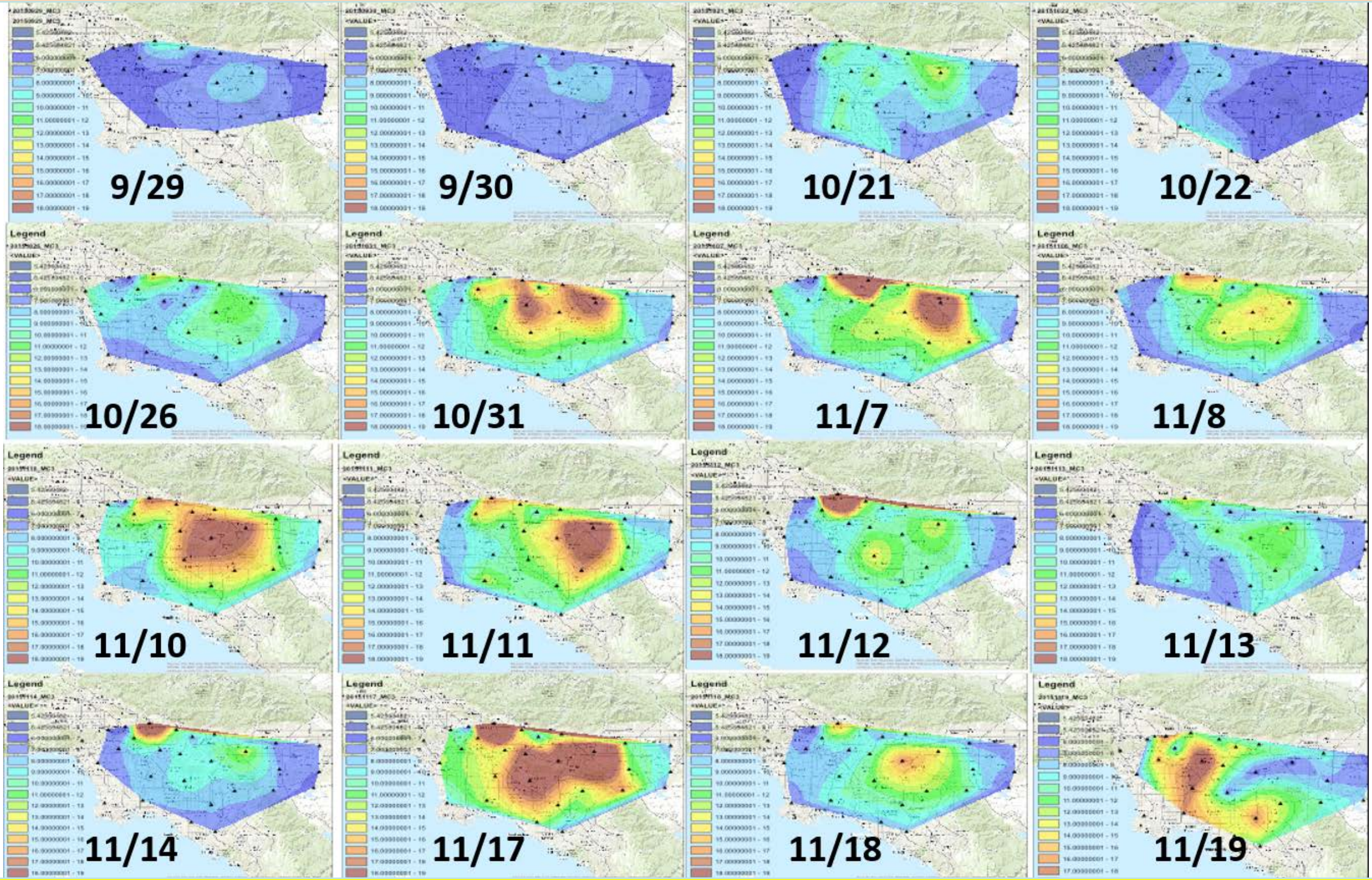

Spatial variability on short time scales demonstrates variability in atmospheric transport

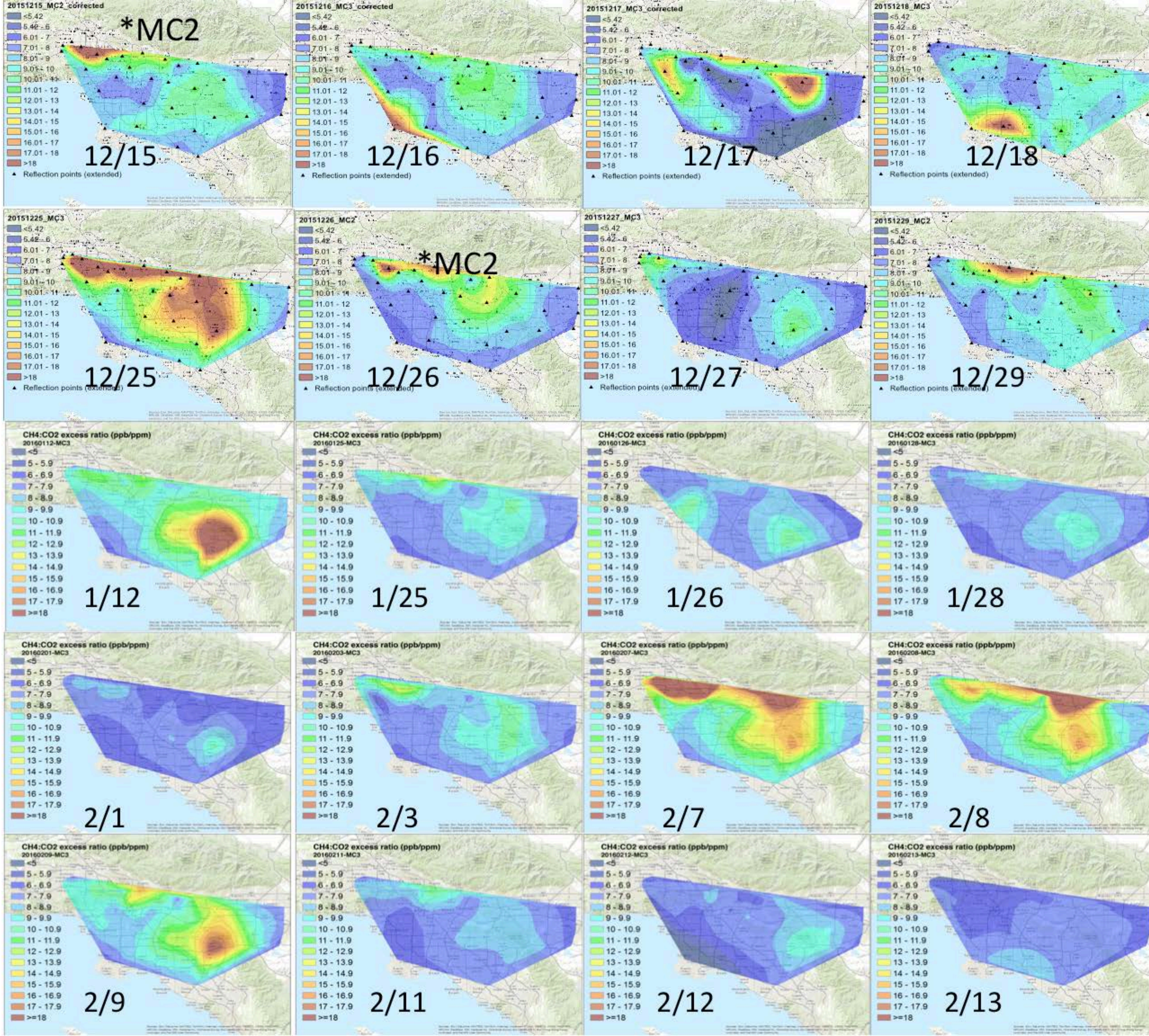

20151215_MC2_corrected
*MC2
12/15
20151216_MC3_corrected
12/16
20151217_MC3_corrected
12/17
20151218_MC3
12/18
<5.42
5.42 - 6
6.01 - 7
7.01 - 8
8.01 - 9
9.01 - 10
10.01 - 11
11.01 - 12
12.01 - 13
13.01 - 14
14.01 - 15
15.01 - 16
16.01 - 17
17.01 - 18
>18
Reflection points (extended)
20151225_MC3
12/25
20151226_MC2
*MC2
12/26
20151227_MC3
12/27
20151229_MC2
12/29
CH4:CO2 excess ratio (ppb/ppm)
20160112-MC3
1/12
20160125-MC3
1/25
20160126-MC3
1/26
20160128-MC3
1/28
<5
5 - 5.9
6 - 6.9
7 - 7.9
8 - 8.9
9 - 9.9
10 - 10.9
11 - 11.9
12 - 12.9
13 - 13.9
14 - 14.9
15 - 15.9
16 - 16.9
17 - 17.9
>=18
20160201-MC3
2/1
20160203-MC3
2/3
20160207-MC3
2/7
20160208-MC3
2/8
20160209-MC3
2/9
20160211-MC3
2/11
20160212-MC3
2/12
20160213-MC3
2/13

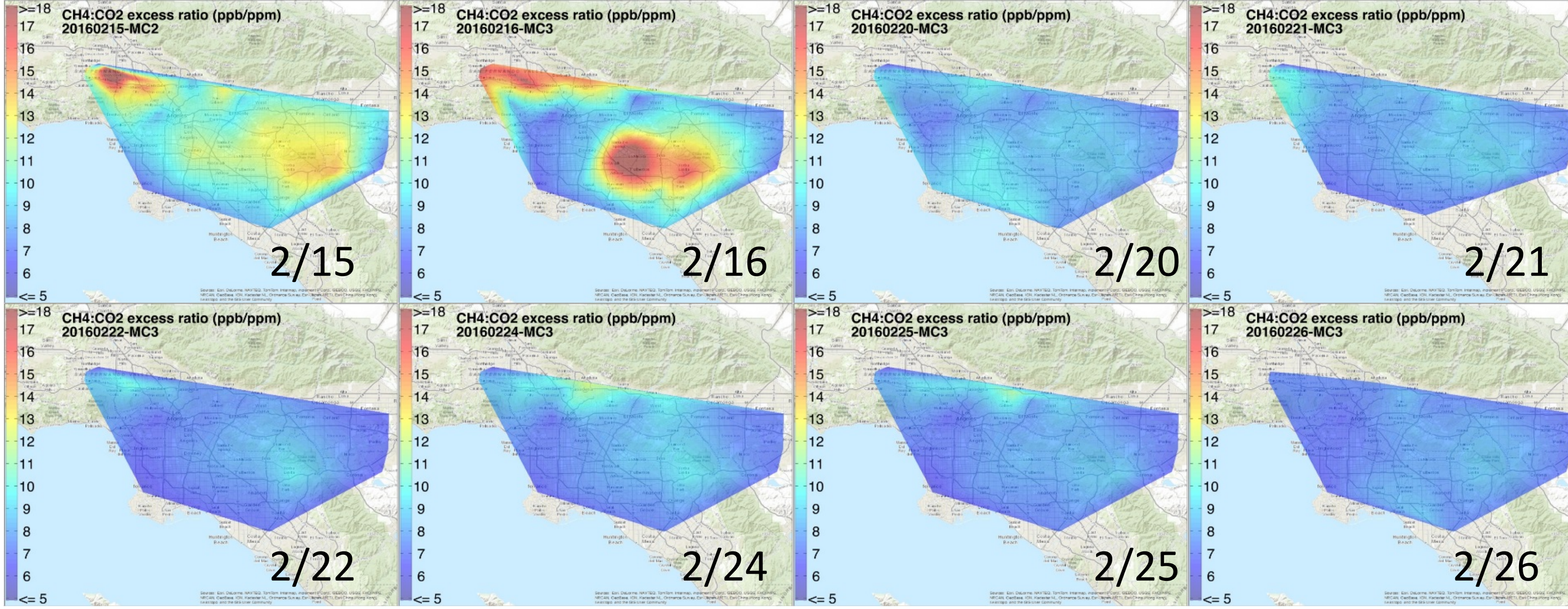

CH4:CO2 excess ratio (ppb/ppm)
20160215-MC2
2/15
CH4:CO2 excess ratio (ppb/ppm)
20160216-MC3
2/16
CH4:CO2 excess ratio (ppb/ppm)
20160220-MC3
2/20
CH4:CO2 excess ratio (ppb/ppm)
20160221-MC3
2/21
CH4:CO2 excess ratio (ppb/ppm)
20160222-MC3
2/22
CH4:CO2 excess ratio (ppb/ppm)
20160224-MC3
2/24
CH4:CO2 excess ratio (ppb/ppm)
20160225-MC3
2/25
CH4:CO2 excess ratio (ppb/ppm)
20160226-MC3
2/26
>=18
17
16
15
14
13
12
11
10
9
8
7
6
<= 5

Estimated CLARS CH_4 flux from SoCAB (6/1/2015 – 3/1/2016)

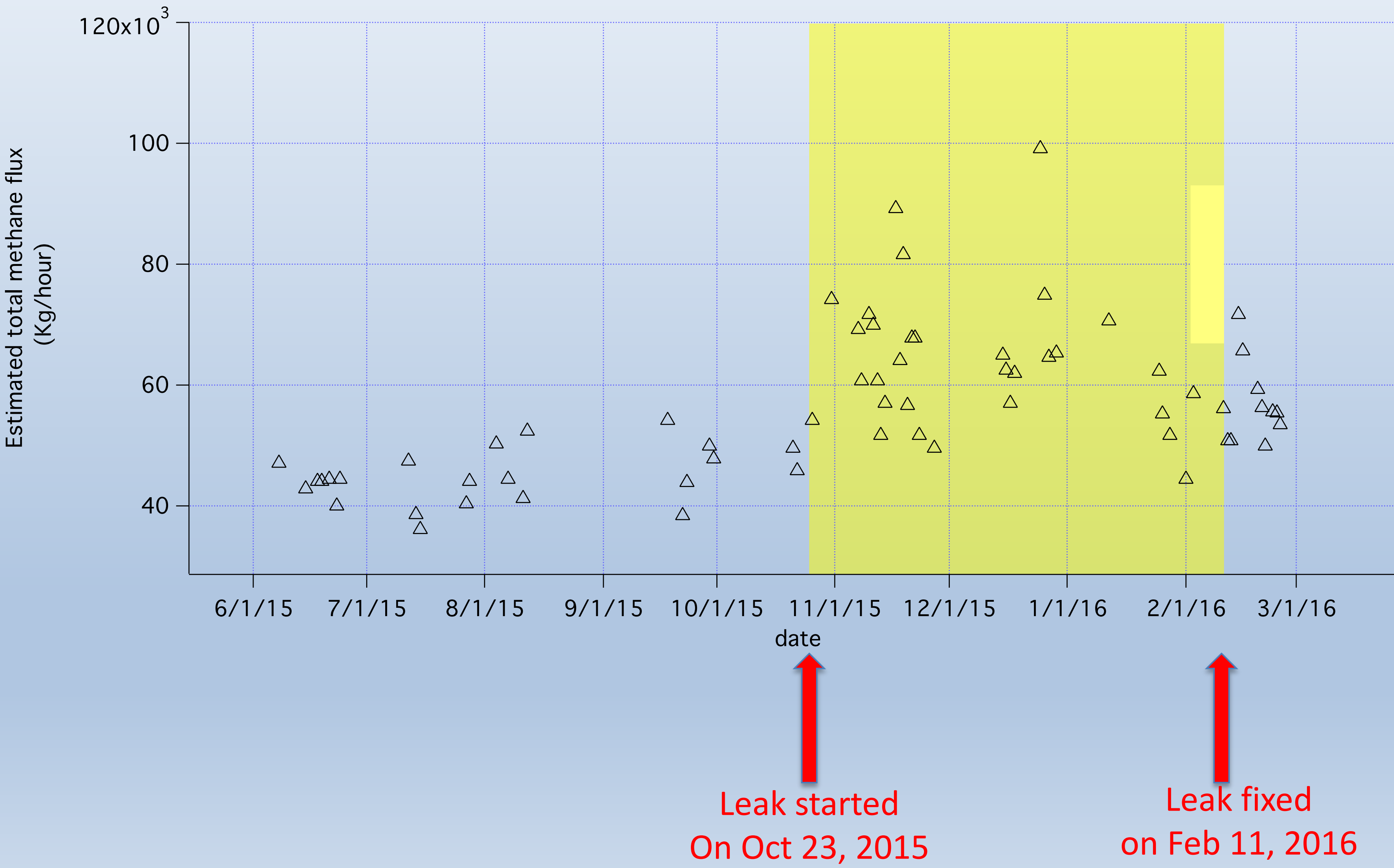

Inferring the Aerosol Vertical Profile from CLARS-FTS O_2 Observations

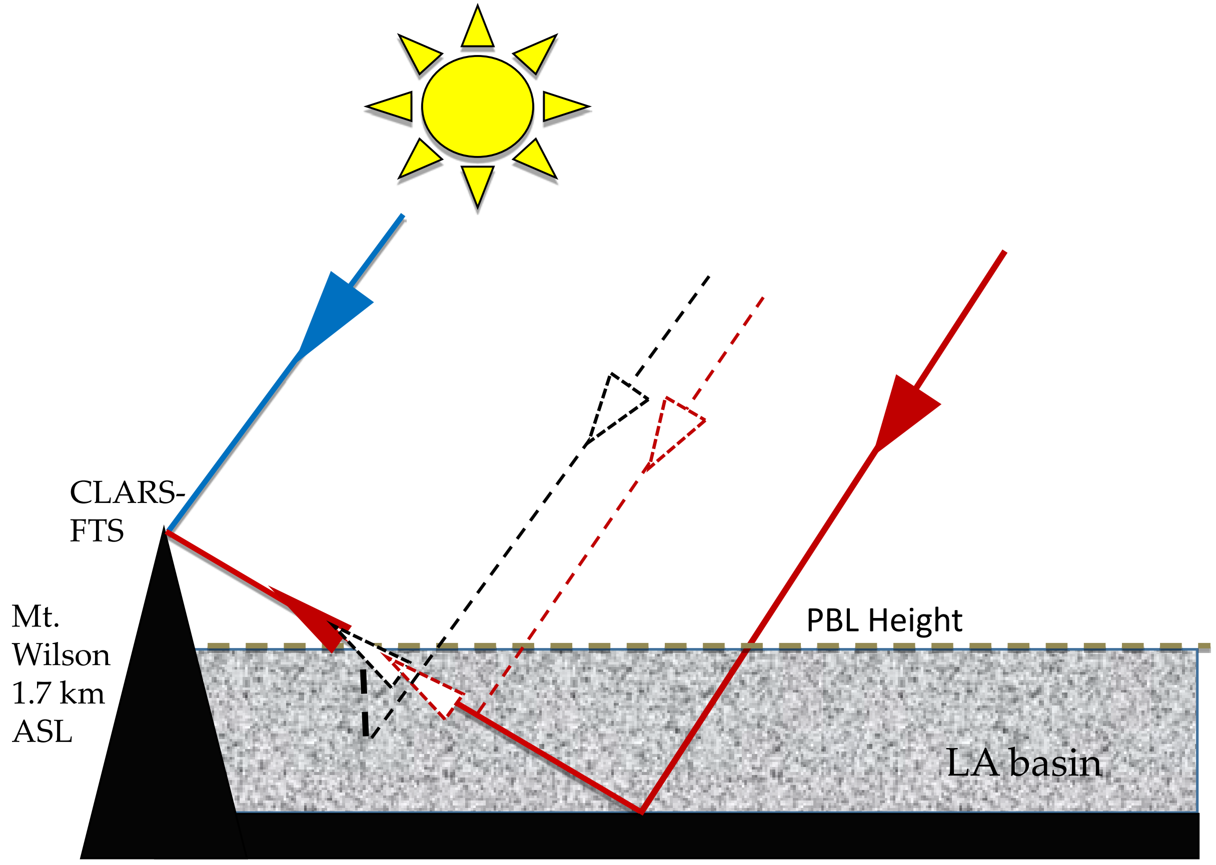

Aerosol scattering

- “Short-circuits” the optical path relative to the surface
- Increases the observed radiance for highly scattering aerosols

Sensitivity of radiance and lineshape to aerosol

3 pm local time

2013-09-25

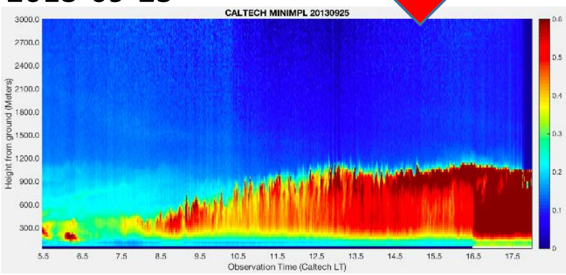

2013-09-24

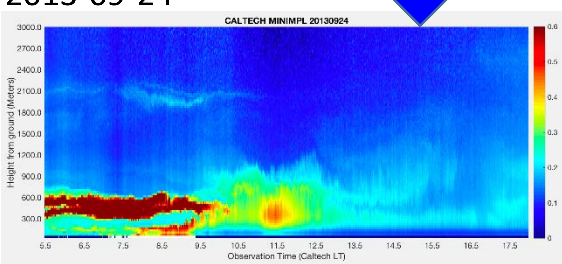

MiniMPL aerosol backscatter at Caltech

Two consecutive days (ensure similar geometries) with different aerosol loadings

Oxygen band at 1.27 um

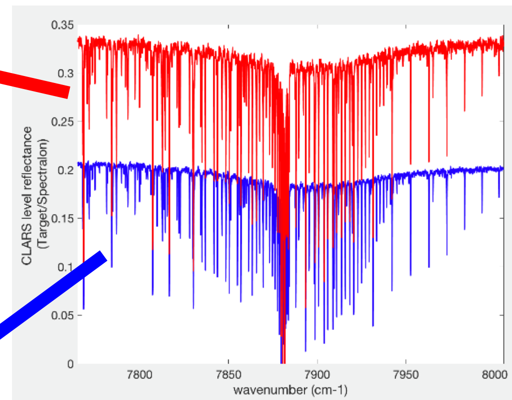

Enhancement in CLARS continuum radiance

Liou (2002)
Richardson et al. (2016)

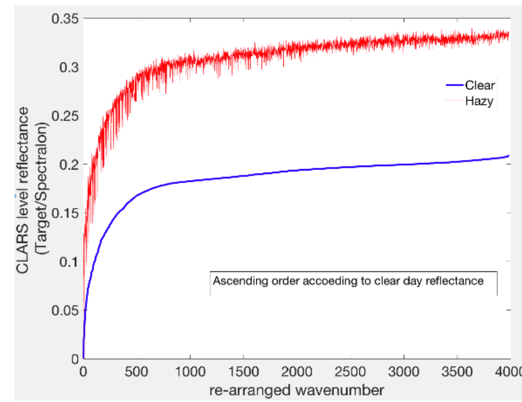

Sorted radiance

- Sort the clear-day radiance and then apply to hazy-day radiance
- The advantage of this sorting will be obvious when studying the impact of aerosol profiles (next slide)

Zeng et al. in preparation (2018)

Retrieval of aerosol vertical profile

A

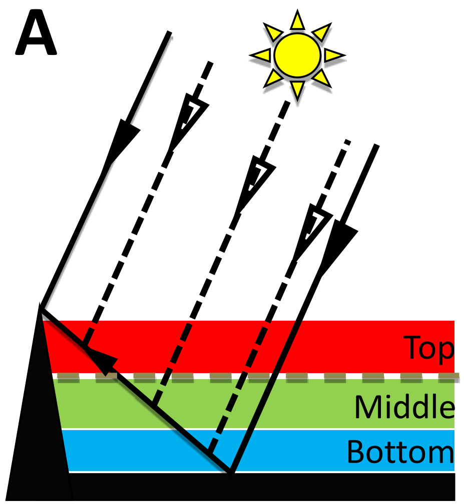

3 scenarios:
Same aerosol loading but at different altitudes

B

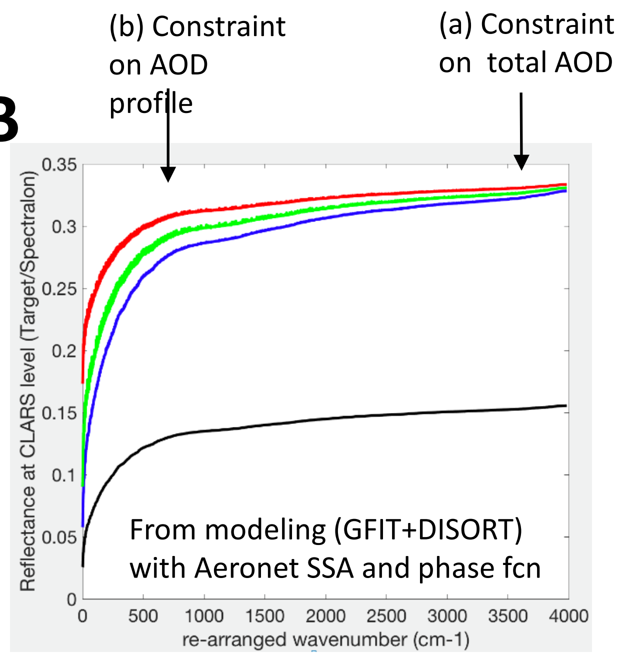

(a) The continuum level doesn't change with aerosol layer height because scattered light is not absorbed;
(b) The effect of scattering in line wings relative to line cores depends on the aerosol layer height.
-> the sorted radiance provides two pieces of information to constrain total and profile AOD

C

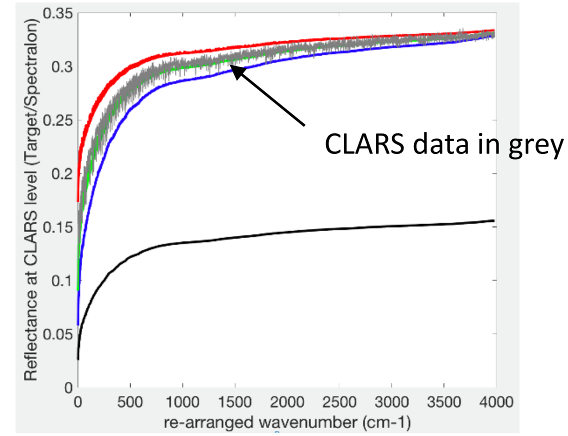

Retrieve the profile by fitting the radiance

D

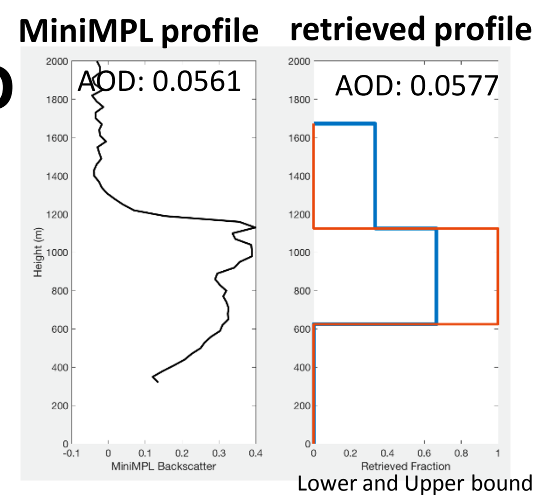

Zeng et al. in preparation (2018)

Geostationary Imaging Fourier Transform Spectrometer: Hourly Sampling of XCO_2, XCH_4, XCO

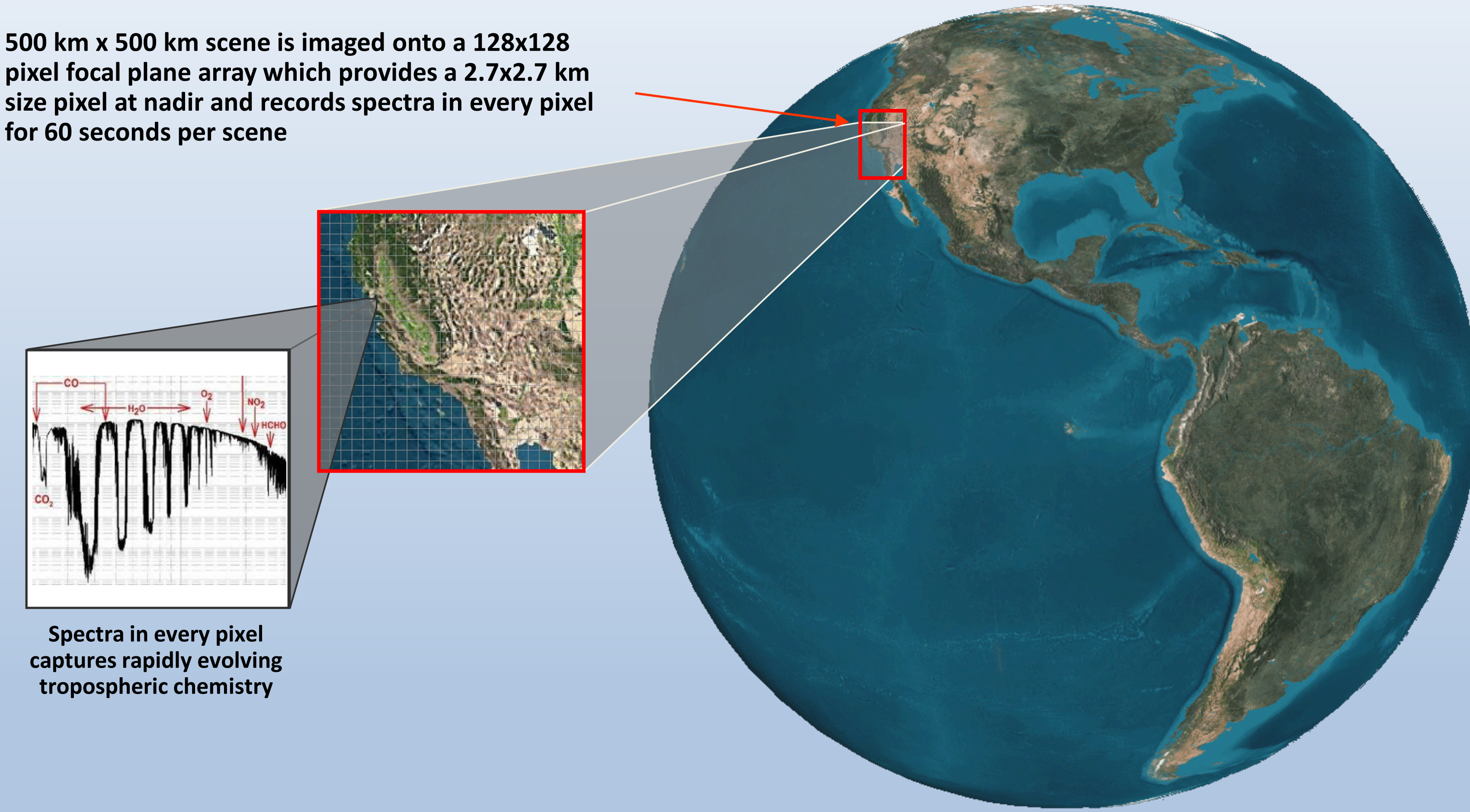

From geostationary orbit GeoFTS can map all of North and South America hourly with high resolution measurements (temporal, spatial, and spectral) that capture rapidly evolving tropospheric concentrations with planetary boundary layer sensitivity

Panchromatic Fourier Transform Spectrometer (PanFTS): Engineering Model for Geostationary Chemical Imaging

- Spectral Coverage: 0.3-10 μm
- 2 Dynamically Aligned Plane Mirror Michelson Interferometers MOPD = 10 cm
- 3 Cameras: 128x128 focal plane arrays with in-pixel digitization
- 2.7 km nadir ground sampling/pixel from geostationary orbit

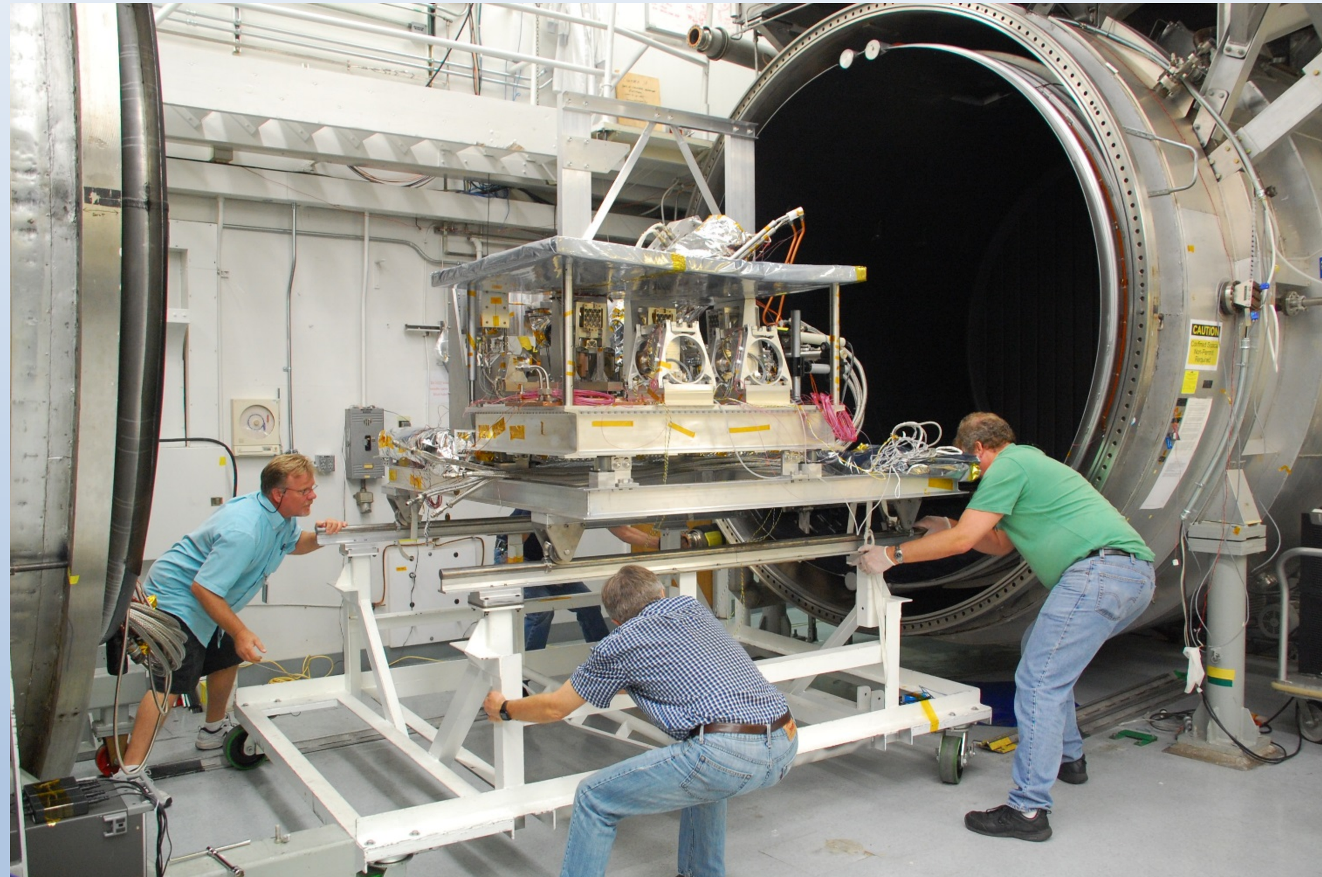

PanFTS Engineering Model being inserted into JPL’s 10-foot thermal-vacuum chamber for environmental testing in vacuum at -100 °C.

GEO-PanFTS Engineering Model Demonstrated in LA

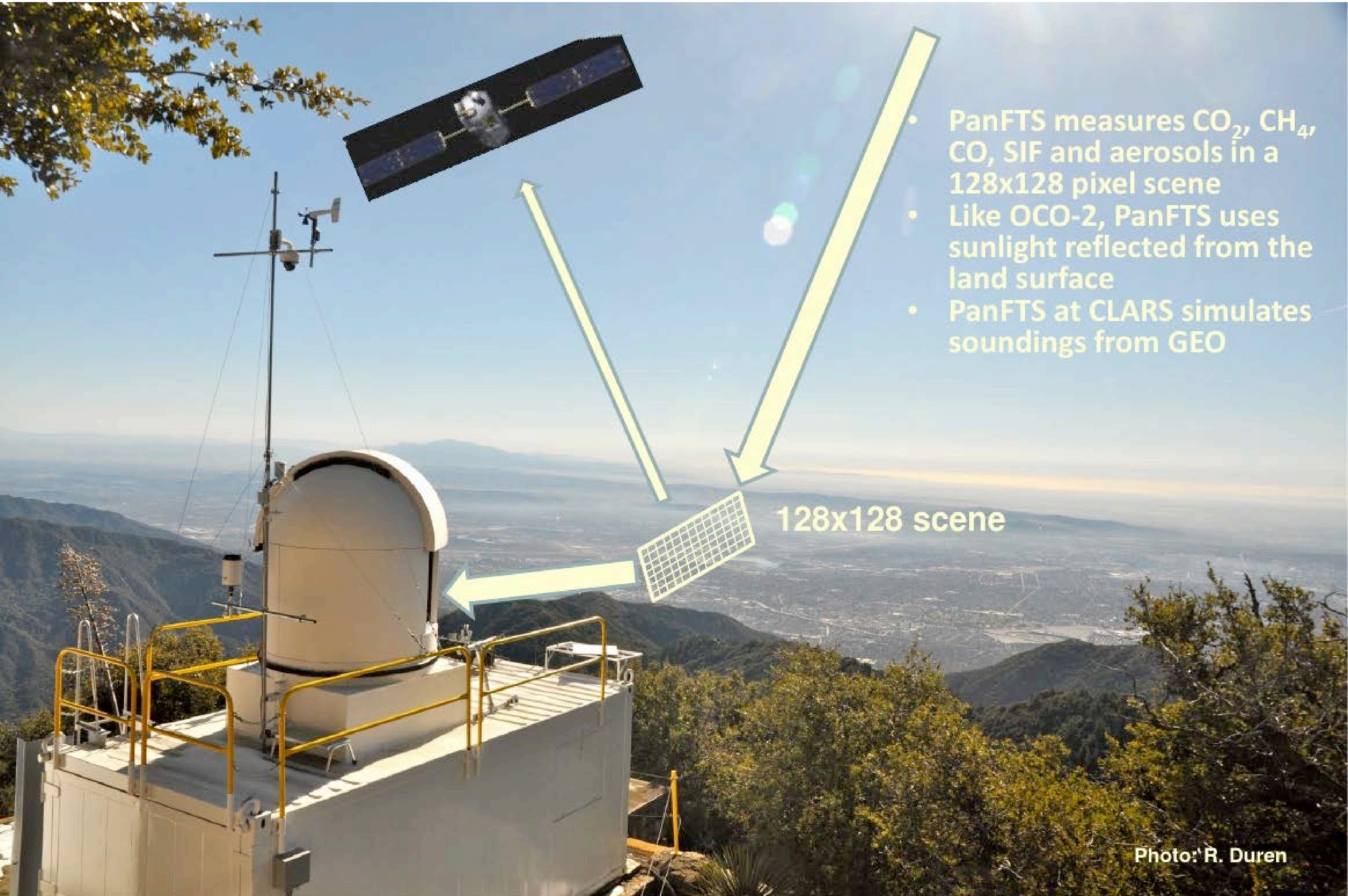

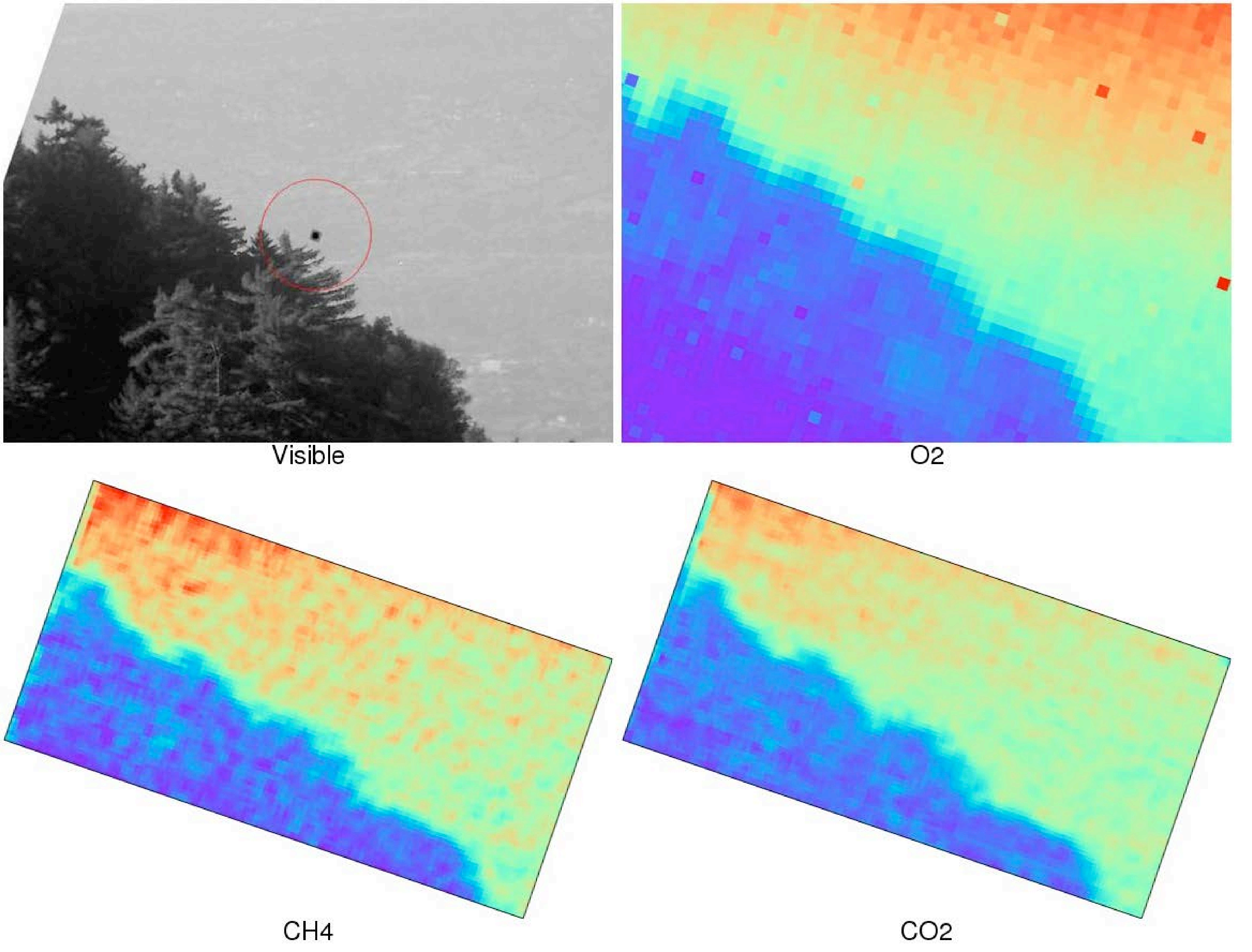
Visible
O2
CH4
CO2

Findings and Recommendations

- Observational data from CLARS, which mimic a geostationary platform, confirm the value of persistent measurements with high temporal, spatial and spectral resolution
- CLARS results on CH_4 show that the additional data volume provided by GEO mapping on dense space-time grids will enable more accurate determinations of regional trace gas fluxes.
- Enables the jump from mapping missions to process-oriented missions.
- Geostationary observations are well-suited to capture rapidly evolving emissions from industrial accidents, hot spots and other episodic emissions such as the Aliso Canyon natural gas well leak.
- A GEO mission/constellation should be an integral part of NASA's mission strategy for the aerosol, trace gas/ozone and greenhouse gas targeted observables in the 2018 Decadal Survey.

Acknowledgements

- GEO-CAPE Pre-Phase A Project for supporting this work
- Jay, Daniel and David for outstanding leadership over the years
- Laura Iraci for outstanding support to the Project in so many ways

Publications Acknowledging GEO-CAPE Support

Zeng, Z.-C., Zhang, Q., Margolis, J. S., Shia, R.-L., Newman, S., Fu, D., Pongetti, T. J., Wong, K. W., Sander, S. P., Wennberg, P. O., and Yung, Y. L.: Investigating wavelength-dependent aerosol optical properties using water vapor slant column retrievals from CLARS over the Los Angeles basin, *Atmos. Chem. Phys.*; **2017**, *17*, 2495-2508. http://dx.doi.org/ 10.5194/acp-17-2495-2017

Wong, K. W.; Pongetti, T. J.; Oda, T.; Gurney, K. R.; Newman, S.; Duren, R.; Miller, C. E.; Yung, Y. L.; Sander, S. P.; Monthly trends of top-down methane emissions in the South Coast Air Basin from 2011-2015; *Atmos. Chem. Phys.*; **2016,** *16,* 9019-9045, http://dx.doi.org/10.5194/acp-16-13121-2016

Feng, S.; Lauvaux, T.; Newman, S.; Rao, P.; Ahmadov, R.; Deng, A.; Diaz-Isaac, L. I.; Duren, R. M.; Fischer, M. L.; Gerbig, G.; Gurney, K. R.; Huang, J.; Jeong, S.; Li, Z.; Miller, C. E.; O'Keefe, D. O.; Patarasuk, R.; Sander, S. P.; Song, Y.; Wong, K. W.; Yung, Y. L.; L.A. Megacity: A high resolution land-atmosphere modeling system for urban CO_2 emissions; *Atmos. Chem. Phys.;* **2016,** *16*, 13121-13130, http://dx.doi.org/10.5194/acp-16-9019-2016

Wong, K. W.; Pongetti, T. J.; Oda, T.; Gurney, K. R.; Newman, S.; Duren, R.; Miller, C. E.; Yung, Y. L.; Sander, S. P.; Monthly trends of top-down methane emissions in the South Coast Air Basin from 2011-2015; *Atmos. Chem. Phys.*; **2016,** *16,* 9019-9045, http://dx.doi.org/10.5194/acp-16-13121-2016

Zhang, Q.; Natraj, V.; Li, K.-F.; Shia, R.-L.; Fu, D.; Pongetti, T. J.; Sander, S. P.; Roehl, C. M.; Yung, Y. L.; Accounting for aerosol scattering in the CLARS retrieval of column averaged CO_2 mixing ratios, *J. Geophys. Res. Atmos.*; **2015**, *120*, 7205-7218, dx.doi.org/10.1002/2015JD023499

Xi, X.; Natraj, V.; Shia, R. L.; Luo, M.; Zhang, Q.; Newman, S.; Sander, S. P.; Yung, Y. L.; Simulated retrievals for the remote sensing of CO_2, CH_4, CO, and H_2O from geostationary orbit, *Atmos. Meas. Tech.*; **2015**, *8*, 4817-4830, dx.doi.org/10.5194/amt-8-4817-2015

Wong, K. W.; Fu, D.; Pongetti, T. J.; Newman, S.; Kort, E. A.; Duren, R.; Hsu, Y-K.; Miller, C. E.; Yung, Y. L.; Sander, S. P.; Mapping CH4:CO2 ratios in Los Angeles, with simulated satellite remote sensing from Mount Wilson, California, Atmos. Chem. Phys., 2015, 15, 241-252, http://doi.org/10.5194/acp-15-241-2015

Fu, D.; Pongetti, T. J.; Blavier, J-F L.; Crawford, T. J.; Manatt, K. S.; Toon, G. C.; Wong, K. W.; Sander, S, P.; Near-infrared remote sensing of Los Angeles trace gas distributions from a mountaintop site, Atmos. Meas. Tech., 2014, 7, 713-729, http://doi.org/10.5194/amt-7-713-2014